

Newcastle University MRes Marine Ecosystems and Governance

Investigating the impacts of the 2017 Hurricane season on the shallow marine environment of the British Virgin Islands using multispectral satellite imagery

Isabel Hassall PGR

i.hassall2@ncl.ac.uk

Supervisor: Dr Clare Fitzsimmons



Acknowledgements

I would like to thank Nancy Woodfield Pascoe, Finfun Peters and the team at The National Parks Trust of the Virgin Islands for facilitating the field data collection. I would like to acknowledge the invaluable contribution of the Joint Nature Conservation Committee. I would also like to thank Environment Systems Ltd, particularly Samuel Pike and Dr Katie Medcalf, for providing satellite imagery data and vital assistance throughout this project. Finally, I would like to thank Dr Clare Fitzsimmons for her continued support and advice throughout this research.

Contents

Abstract	2
Introduction	2
Caribbean Ecosystems	3
Recovery Potential	3
Remote Sensing in Coastal Environments	3
Satellite Derived Bathymetry	4
Benthic Habitat Classification	5
Change Detection	7
2017 Caribbean Hurricane Season	8
Rationale	8
Project Aims	8
Objectives	8
Methods	9
Site Description	9
Data	10
Ground-Truth Data Collection	14
Image Pre-Processing	15
Bathymetry Derivation	18
Habitat Mapping	19
Change Detection	21
Results	21
Bathymetry	21
Habitat	27
Discussion	33
Image Pre-Processing	33
Satellite Derived Bathymetry	33
Habitat Mapping	34
Change Detection	35
Limitations	35
Future Study	36
Conclusion	37
References	38
Appendix A: Image Parameter Tables	41
Appendix B: Preliminary Ground-Truth Site Selection	42
Appendix C: Habitat Classification Stability	45

Abstract

Hurricanes have intense destructive impacts on biodiverse and valuable shallow-water ecosystems of the Caribbean. Quantifying and mapping the spatial distribution of these impacts assists marine management efforts. This paper utilises satellite imagery techniques to derive bathymetry and benthic habitat cover of the British Virgin Islands (BVI) before and after Hurricane Irma in September 2017. The robust ratio transform approach was applied to WorldView-2 images to generate bathymetry data and Object-Based Image Analysis (OBIA) methods provided habitat maps for the pre and post-Irma scenes. Change detection analyses identified the location and magnitude of change across the archipelago. Depth and habitat models were validated with independent ground-truth data obtained via multibeam echosounder (MBES) surveys and field data collection. Satellite-Derived Bathymetry (SDB) models achieved Root Mean Square Error (RMSE) values of 2.42m and 3.84m and Mean Absolute Error values of 0.078m and 0.44m (MAE) for the pre and post-Irma scenes respectively. Pre and post-Irma habitat maps were 62% and 67% accurate respectively. Change detection identified significant differences in depth between the pre and post-Irma scenes. Research outputs assess the influence of Hurricane Irma on the shallow-water environment of the BVI and provide a baseline for future ecological monitoring programmes. This paper reinforces the merit of remote sensing systems in bathymetry and habitat mapping and highlights the great potential of these techniques in assessing changes to the marine environment.

Introduction

Shallow-water ecosystems, such as coral reefs and seagrass beds, provide invaluable ecosystem services and are biodiversity hotspots. Millions of people worldwide, particularly in developing countries, depend on reef ecosystems for fisheries, tourism, coastal protection (Cinner *et al.*, 2016) while seagrass beds stabilise coastal sediments, improve water quality and provide nursery and feeding grounds for fish and turtle species (Topouzelis *et al.*, 2016).

But they are under severe pressure from human populations and are vulnerable to extensive damage from natural disasters. Nutrient enrichment, overfishing and elevated sea temperatures are examples of chronic stressors undermining the recovery potential of marine ecosystems following natural disturbances (Alvarez-Filip *et al.*, 2011; Bythell *et al.*, 2000).

Hurricanes pose a significant threat in the coastal environment. These powerful events trigger excessive nutrient loading, fish mortality, algal blooms, the release of pathogens and pollutants in addition to mechanical destruction of coral structures and scouring of seagrass beds (Klemas, 2009; Mumby, 1999). Although Hurricanes play a relatively small role in global coral cover declines, these events have substantial localised impacts and can inflict damage up to 50m deep (Alvarez-Filip *et al.*,

2011). The majority of the destruction is felt within 10-20m depth, where coral breakage and abrasion is most intense and the near-total removal of benthic communities can occur (Hubbard *et al.*, 1991). Hurricanes drive major reductions in coral reef complexity following mass mortality of more delicate branching species, which alters the ecosystem dynamics and lowers biodiversity (Alvarez-Filip *et al.*, 2011; Bythell, 1997).

Caribbean Ecosystems

Caribbean coastal ecosystems are some of most threatened habitats in the world. The synergistic effects of chronic human stressors, intense Hurricane impacts and mass mortality events of *Acropora palmata* and *Diadema antillarum* in the 1970s and 1980s respectively have decimated Caribbean reefs (Bythell *et al.*, 2000; Hoegh-Guldberg *et al.*, 2007). Coral cover has declined by 80% over the last four decades (Gardner *et al.*, 2003). Phase-shifts to algal dominance are prevalent throughout the Caribbean (Hoegh-Guldberg *et al.*, 2007) and are facilitated by the clearing of substrate during Hurricane events. Hurricane induced scouring and boat anchor scars are rife in Caribbean seagrass beds (Short *et al.*, 2011).

In 1989 Hurricane Hugo reduced coral cover to 0.8% in shallow areas of the Buck Island Reef National Monument, St Croix (Rogers, 2000). Caribbean coral cover is reduced by an average of 17% the year following a Hurricane and impacted sites continue to decline at a faster rate than sheltered areas, highlighting the lasting effects of these events (Gardner *et al.*, 2005). Up to 11% of the historical extent of Caribbean reefs were lost by 2003, with 16% significantly damaged (Gardner *et al.*, 2003). The rate of decline has slowed since the 1980s, but the negative trend persists (Gardner *et al.*, 2003). The significant degradation of Caribbean shallow-water ecosystems and the continued negative change trajectory highlights the urgent need for effective management.

Recovery Potential

Coastal ecosystems have high recovery potential following natural disasters. Coral cover in St Croix, US Virgin Islands, recovered to 89% of the pre-Hurricane Hugo levels within six years (Bythell, 1997) while species richness increased to 136% of the pre-Hurricane levels following the category 5 event (Bythell *et al.*, 2000). However, underlying anthropogenic pressures hinder the natural recovery mechanisms of coral reefs (Hughes, 1994). These seminal studies are fairly outdated, which highlights the need for current research into Hurricane impacts on coastal ecosystems.

Remote Sensing in Coastal Environments

Bathymetry estimations further our understanding of the oceanographic processes underlying marine ecosystem dynamics (Traganos *et al.*, 2018). Bathymetric data are required for navigation, assessing sediment movements and examining the complexity of marine habitats (Hernandez and Armstrong,

2016; Jagalingam *et al.*, 2015). Mapping the spatial distribution of benthic habitats identifies ecosystems vulnerable to disturbance events and highlights target areas for conservation measures. Combining bathymetric and benthic cover data creates a holistic view of the near-shore environment. Bathymetry and habitat extent assessments form the basis of change detection studies, both in response to a discrete event and as part of an extended time-series.

The extensive and often inaccessible nature of coastal environments coupled with the prohibitive costs of conventional in-situ data collection restricts the provision of accurate baseline data for long-term monitoring programmes (Jagalingam *et al.*, 2015). Developments in active sensors, such as LiDAR and sonar devices, are useful in bathymetry detection, but these methods cover relatively small areas, are time-consuming and extremely costly (Evagorou *et al.*, 2019). The application of satellite based remote sensing in the marine environment creates new research opportunities, as the vast area covered by a single image and comparatively low acquisition costs make this resource invaluable and accessible.

The launch of the first Landsat platform and seminal research in the 1970s and 1980s identified the great potential of remote sensing techniques for marine mapping (Lyzenga 1978; 1981; Schott *et al.*, 1988). Further developments in image pre-processing and SDB algorithms led to vast improvements in mapping accuracies (Mumby *et al.*, 1998; Stumpf *et al.*, 2003). Increased image spatial resolution enables the interpretation of fine details in complex marine ecosystems, such as coral reefs (Call *et al.*, 2003).

Satellite Derived Bathymetry

SDB has the capacity to provide accurate baseline data for change detection analyses and long-term monitoring schemes on a large scale. Detailed bathymetric data provides information about the complexity of shallow-water reefs, which can be assessed at different time scales to identify structural change (Hedley *et al.*, 2018). Current SDB methods are divided into analytical and empirical approaches (Pe'eri *et al.*, 2014).

Two competing approaches are driving developments in interpretation. Analytical methods are based on radiative transfer models and require estimates of atmospheric, water column and bottom material parameters (Pe'eri *et al.*, 2014; Gao, 2009). Physics-based optimisation approaches deconstruct spectra into components relating to water depth, quality and benthic cover (Hamylton *et al.*, 2015).

Empirical methods are simplified models with fewer parameters. Concurrent depth measurements are needed to train these models and the accuracy of SDB estimates is heavily dependent on water

depth (Gao, 2009; Hamylton *et al.*, 2015). However, successful bathymetry data has been calculated up to 20m depth in many previous studies (Evagorou *et al.*, 2019; Hochberg *et al.*, 2003; Pe'eri *et al.*, 2014).

One effective approach was pioneered by Lyzenga (1978; 1981), based on the idea that bottom-reflected radiance is a linear function of bottom reflectance and an exponential function of depth. The Lyzenga (1978) linear transform method provides a relationship between reflectance, depth and bottom albedo. This method performs well but requires the estimation of five variables and struggles to retrieve depths beyond 15m deep and in areas of low bottom albedo (Stumpf *et al.*, 2003).

The ratio transform method outlined by Stumpf *et al.* (2003) solves these difficulties by using the ratio of two spectral bands to infer depth. This approach works on the principle that spectral radiation is attenuated through the water column and relies on the idea that bottom radiance of one band decays at a faster rate than the other (Pe'eri *et al.*, 2014). The reflectance of the spectral band with higher absorption will decrease proportionately faster than the band with the lower absorption (Stumpf *et al.*, 2003). A widely-used band combination is blue:green, as green light is absorbed more quickly than blue light as depth increases, meaning the ratio of blue:green increases with depth (Stumpf *et al.*, 2003). The high penetration depth of the blue band increases the potential for extracting depth information (Caballero and Stumpf, 2019). The Stumpf *et al.* (2003) method assumes the water column is uniformly mixed and affects the reflectance of both bands similarly (Pe'eri *et al.*, 2014). The ratio transform approach compensates for variable bottom habitat type, as changes in albedo associated with different benthic cover types will affect both bands similarly, whereas changes in depth will influence the green band more than the blue band (Stumpf *et al.*, 2003). The SDB model is trained and validated using ground-truth depth measurements (Lee *et al.*, 2013; Gao, 2009).

Both linear and ratio transform methods are effective, but the ratio transform approach is less complex, retrieves depths of over 25m in clear waters and shows greater stability than the linear transform method (Stumpf *et al.*, 2003).

Benthic Habitat Classification

Identifying benthic habitat cover supports and builds upon bathymetric data in mapping diverse coastal environments. The benthic cover of an area influences the surface-leaving reflectance used in SDB (Doxani *et al.*, 2012). Habitat maps can improve the training of SDB models over variable bottom-type and validate SDB complexity information using genuine benthic cover data. Previous research has shown the aptitude of remote sensing methods in mapping seagrass percentage cover, species composition, biomass and area extent, making it a valuable tool in marine planning and monitoring (Fauzan *et al.*, 2017; Phinn *et al.*, 2008).

Depth Invariant Index Creation

The confounding influence of variable depth on the bottom reflectance poses difficulties in habitat mapping (Mumby *et al.*, 1998). In order to correct for the effects of the water column on bottom reflectance a Depth Invariant Index (DII) is created, as outlined by Lyzenga (1978; 1981). The gradient of the regression line between two visible bands give the ratio of attenuation coefficients, which are used to generate a DII (Manessa *et al.*, 2014). The DII is used as the input for classification processes, as the variation in bottom reflectance is assumed to be a result of bottom albedo alone (Lyzenga, 1981; Manessa *et al.*, 2014; Hafizt *et al.*, 2017).

Classification

There are multiple different methods used to classify satellite images to derive meaningful information about the extent of underwater habitats. Classification algorithms are commonly applied on a pixel level, but the recent development of object-based image analysis (OBIA) provides an alternative approach. In pixel-based approaches, multiple habitat types often fall within a single pixel, restricting the distinction between bottom-types (Wicaksono, 2016). OBIA clusters smaller pixels into image objects using spectral signatures and pixel shape and size (Wicaksono, 2016). This enhances the ability to create habitat maps using object statistics that are meaningful at real-world habitat scales.

Pixel-based Approach

Unsupervised classification methods are the most basic and are often used to create preliminary habitat classes for planning field surveys (Halls and Costin, 2016; Pu *et al.*, 2012). Unsupervised algorithms generate a specified number of classes by clustering pixels with similar spectral signatures that the user then assigns to meaningful habitat classes (Halls and Costin, 2016). Popular algorithms include K-Means and ISODATA.

Supervised classification methods utilise ground-truth datasets to train and validate the classification process. The most widely-used algorithm is the Maximum Likelihood Classifier, which estimates the probability that a pixel belongs to a certain class (Pu *et al.*, 2012; Halls and Costin, 2016; Manessa *et al.*, 2014). The Maximum Likelihood Classifier performs better than any other parametric classifier, as it takes into account the variance within each class (Koedsin *et al.*, 2016). The Mahalanobis Distance Classifier is also popular in habitat mapping (Meyer and Pu, 2012) and machine-learning approaches such as the Support Vector Machine algorithm are becoming more prevalent (Moniruzzaman *et al.*, 2019; Marcello *et al.*, 2018).

Object-based Approach

Many studies suggest that object-based analysis is more accurate and efficient when identifying habitat classes over heterogeneous land cover (Anggoro *et al.*, 2018). OBIA involves segmenting the images into objects using the spectral signatures of pixels to discriminate habitat cover extents (Anggoro *et al.*, 2018; Moniruzzaman *et al.*, 2019). These image objects are then classified using ground-truth data and validated using independent habitat cover points (Moniruzzaman *et al.*, 2019). Additional information can be incorporated into OBIA, such as texture, shape, size and external datasets including bathymetry, slope and aspect, to assign meaningful classes to image objects (Wicaksono, 2016).

Change Detection

Accurate change detection is crucial in understanding the impacts of natural disasters and human pressures on ecosystems (Lu *et al.*, 2004). The outputs of satellite imagery analysis provide the data required for change detection studies. The high revisit frequency of WorldView-2 at 1.1 days enables the regular collection of data for use in long-term monitoring studies and measuring changes following discrete disturbances. Remote sensing allows the assessment of Hurricane damage to optimise future conservation strategies (Klemas, 2009). Using remote sensing techniques to assess land cover change is well documented (Lambin and Strahler, 1994) but this approach is comparatively unexplored in marine settings.

Conventional methods of change detection include image differencing, Principle Components Analysis (PCA) and post-classification comparison (Lu *et al.*, 2004). There has been a diversification of change detection methods in recent years, with new techniques such as Spectral Mixture Analysis and Artificial Neural Networks providing alternatives to traditional procedures (Lu *et al.*, 2004). The incorporation of Geographical Information Systems in remote sensing data analysis is becoming more prevalent (Lu *et al.*, 2004). Many studies highlight the tendency of change detection methods to overestimate changed areas, which poses challenges when interpreting the results (Li and Yeh, 1998).

2017 Caribbean Hurricane Season

Predicted increases in Hurricane intensity and frequency pose a significant threat to shallow marine ecosystems, which highlights the urgent need for effective assessments of Hurricane damage and ecosystem recovery potential (Mann and Emanuel, 2006; Knutson *et al.*, 2010). The BVI has suffered from ten Hurricanes in the 30 years since Hurricane Hugo in 1989, the first event for over 50 years. The 2017 season was unprecedented in its severity with six major events including Hurricanes Irma and Maria, which were both category 5. Hurricane Irma was the most intense and destructive to ever

hit BVI, as the eye passed directly over the islands and winds reached over 170mph (National Hurricane Centre). Hurricane Maria followed closely, limiting the available recovery time.

Rationale

This research will quantify the change in reef and seagrass environments resulting from the 2017 Caribbean Hurricane season and provide a framework for future assessment. The 2014 Darwin Plus project provided bathymetric and habitat cover data for a small area of Tortola (Figure 4) using MBES surveys. More extensive mapping of the BVI marine habitats feeds into the Darwin Plus programme, which aims to establish an ongoing monitoring scheme to analyse the health coral reefs and seagrass beds. Assessing the impacts of discrete Hurricane events and monitoring long-term ecosystem changes provides useful information for marine management policies and helps to identify priority sites for conservation efforts (Topouzelis *et al.*, 2018). This research is one of the first projects to assess Hurricane impacts using satellite imagery techniques.

Project Aims

This research aims to analyse and map the shallow water environment surrounding the BVI using high resolution satellite imagery. Bathymetric and habitat cover maps will be created and the impacts of the 2017 Hurricane season will be identified by comparing the bathymetry and habitat cover of pre-Hurricane and post-Hurricane imagery.

Objectives

- 1) Determine the bathymetry and habitat cover pre-Hurricane Irma;
- 2) Determine the bathymetry and habitat cover following Hurricane Irma;
- 3) Ground-truth the post-Hurricane data using in-water survey techniques;
- 4) Assess the change in bathymetry and habitat cover as a result of the Hurricane season;
- 5) Produce detailed maps of the marine environment in the BVI as the baseline for future long-term monitoring schemes.

Research will utilise the Stumpf *et al.* (2003) ratio transform method of satellite derived bathymetry to produce depth data for the BVI archipelago. OBIA techniques will be applied to determine the extent of major benthic habitat types and Hurricane impacts will be measured using change detection procedures. The literature review and previous related research by Environment Systems and Newcastle University justified the use of these approaches to produce accurate results.

Methods

Site Description

The British Virgin Islands (BVI) are a British overseas territory in the Caribbean Sea. The islands lie at the north-eastern point of the Greater Antilles with Puerto Rico to the west, and include Tortola, Virgin Gorda, Jost Van Dyke, Anegada and 32 smaller islands (Figure 1). Covering an area of 59 square miles they have a population of 28,054 people. The shallow water environment of the BVI is comprised of dense reefs of *Plexauridae*, *Faviidae* and *Montastrea* species with associated soft corals, seagrass meadows of *Syringodium filiforme* and *Thalassia testudinum*, sandy areas and bare coral rubble and rock (Fitzsimmons *et al.*, 2016). Coastal ecosystems of the BVI are threatened by Caribbean-wide pressures such as anthropogenic development, overfishing, pollution and natural events including Hurricanes and climate change (Forster *et al.*, 2011). Prior to the 2017 Hurricane season the reefs of the BVI were considered generally healthier than most in the Caribbean, with consistently high coral cover compared to algal cover (Fitzsimmons *et al.*, 2016). Post-Hurricane assessments have yet to be made, but the health of coral reefs and seagrass beds are expected to have deteriorated.

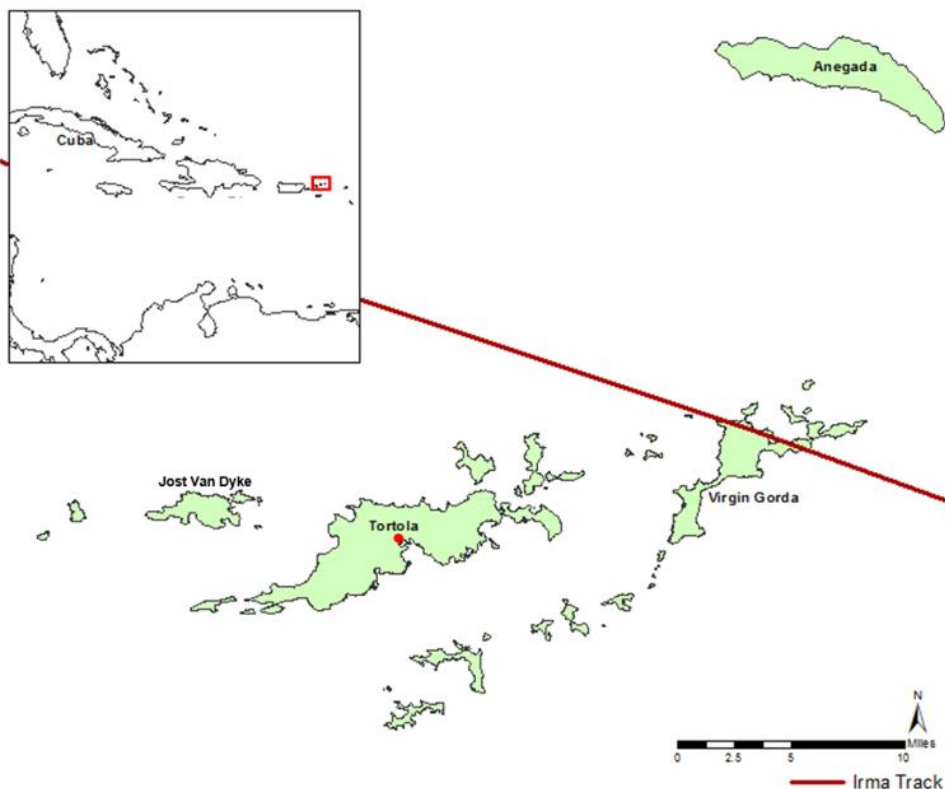


Figure 1: Map of the BVI showing the track of Hurricane Irma. Tortola is the main island and the capital Road Town is denoted by the red circle.

Data

Satellite Imagery Data

Both pre and post-Hurricane image datasets were acquired from DigitalGlobe's WorldView-2 satellite. WorldView-2 offers high resolution imagery and includes additional bands that are expected to improve mapping accuracy (Diedda and Sanna, 2012; Halls and Costin, 2016). Satellite parameters are summarised in Table 1.

Table 1: WorldView-2 satellite image product details.

Satellite Parameter		
Image Type	Standard 2A	
Pixel Size	2.0	
Spatial Resolution	Multispectral 1.85m at nadir; 2.07m at 20° off-nadir Panchromatic 0.46m at nadir; 0.52m at 20° off-nadir	
Radiometric Resolution	16 bits per pixel	
Spectral Bands	Spectral Band	Wavelength (nm)
	Coastal	400 – 450
	Blue	450 – 510
	Green	510 – 580
	Yellow	585 – 625
	Red	630 – 690
	Red Edge	705 – 745
	NIR1	770 – 895
	NIR2	860 – 1040
Swath Width	16.4 km at nadir	
Geographic Coordinate System	WGS_1984	
Projected Coordinate System	WGS_1984_UTM_Zone_20N	

Pre-Irma Images

Newcastle University obtained seven DigitalGlobe WorldView-2 satellite images covering the entire BVI archipelago in 2015 (Figure 2). Six images were used to establish the bathymetry and benthic habitat cover before Hurricane Irma. Cloud cover ranged from 0.1-2.0% and the sun elevation varied between 43.8-54.3° (Appendix A: Table 1).

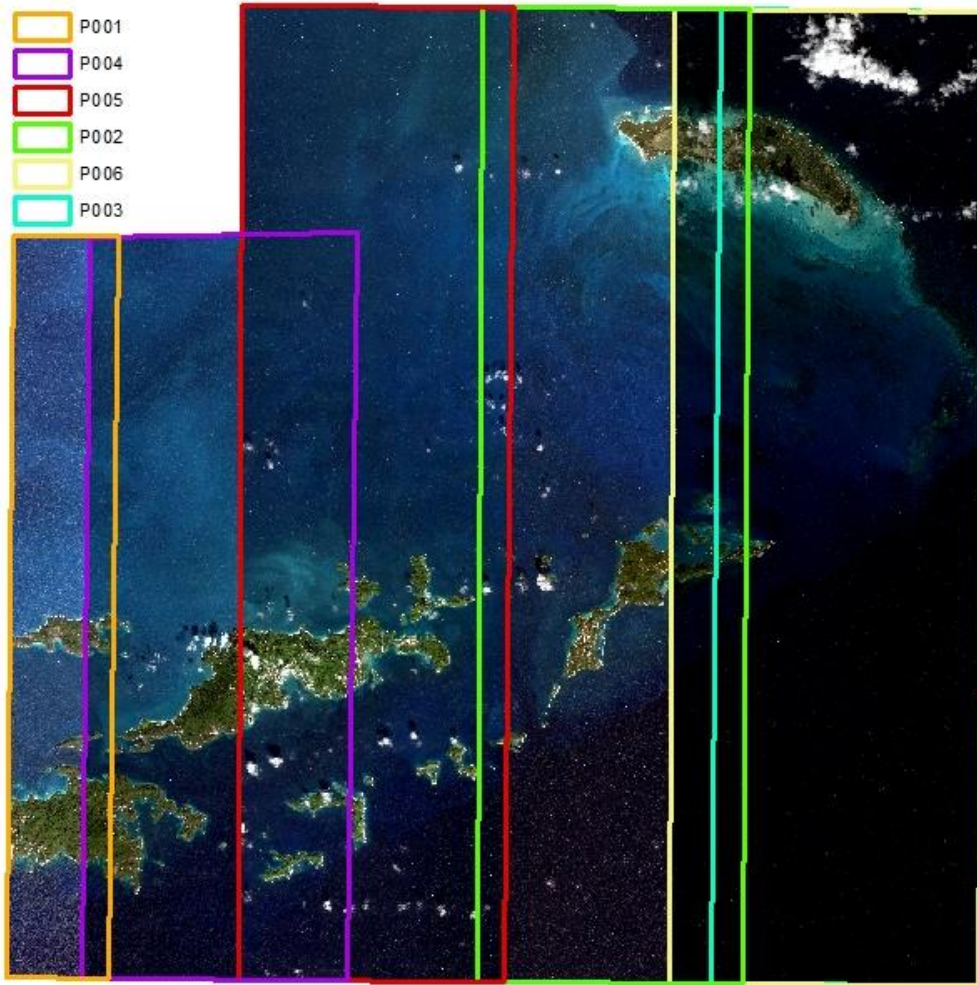


Figure 2: Pre-Irma WorldView-2 satellite images in raw format obtained by Newcastle University.

Post-Irma Images

Six WorldView-2 images taken after Hurricane Irma were obtained by Environment Systems Ltd. and were used to determine the bathymetry and habitat cover following the event (Figure 3). Five images were used, with cloud cover ranging from 4-29.4% and sun elevation between 58.6-73.4° (Appendix A: Table 2).

Anegada was excluded from this research due to a lack of ground-truth data. P005 was used as the reference image for the pre-Irma scene and P001 for the post-Irma scene, as these images contained the most ground-truth points. The pre-Irma ground-truth data only fell within the boundaries of P005 so training and validation points were created in the overlap of images and each image was trained using P005 as the reference. 50% of the ground-truth data points were used as the training dataset and 50% for validation (Phinn *et al.*, 2008). The number of training and validation points for each image varied according to cloud cover and image size. These are summarised in Appendix A: Table 3.



Figure 3: Post-Irma WorldView-2 images in raw format obtained by Environment Systems Ltd.

Ground-Truth Data

Pre-Irma MBES and Still Image Ground-Truth Data

Training and validation data for the Pre-Irma scene were acquired from CEFAS Data Hub. CEFAS conducted bathymetric and benthic habitat surveys as part of the Darwin Plus project DPLUS026 in 2014. Pre-Irma bathymetry was obtained from the raster file “HI1462_MB_Bathymetry_1m.img” and benthic cover data were provided by “DPLUS026_BVI_Proforma_Still_Image_Analysis.csv” and “BVI_Still_Images_Analysis.csv.” MBES bathymetry and still image locations are shown in Figure 4 and the range of depth values is displayed in Figure 5.

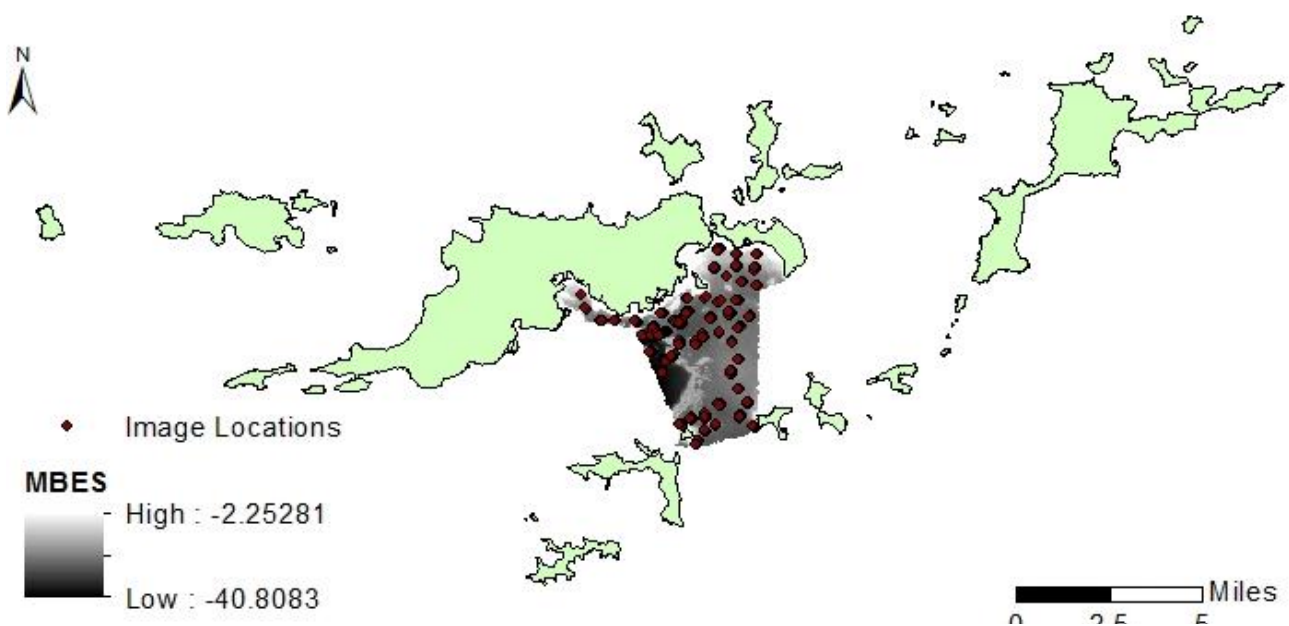


Figure 4: CEFAS ground-truth dataset including MBES bathymetry and still images.

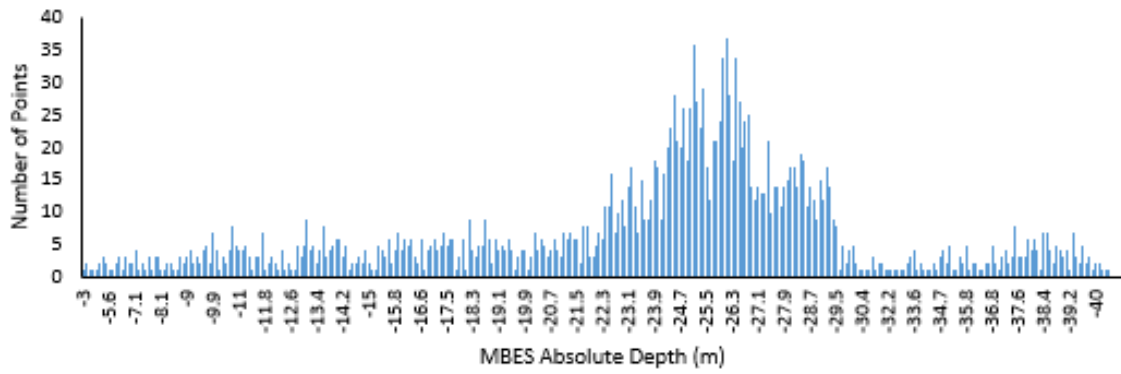


Figure 5: Count of pre-Irma MBES training points for each depth.

Post-Irma Field Survey Ground-Truth Data

An extensive field survey was conducted in June/July 2019 covering the extent of the BVI archipelago, except for Anegada (Figure 6). Georeferenced depth measurements (Figure 7) and underwater still images were taken at each survey site to generate benthic habitat cover data, using Coral Point Count (CPCe) to classify images according to the classification scheme outlined in Figure 8.

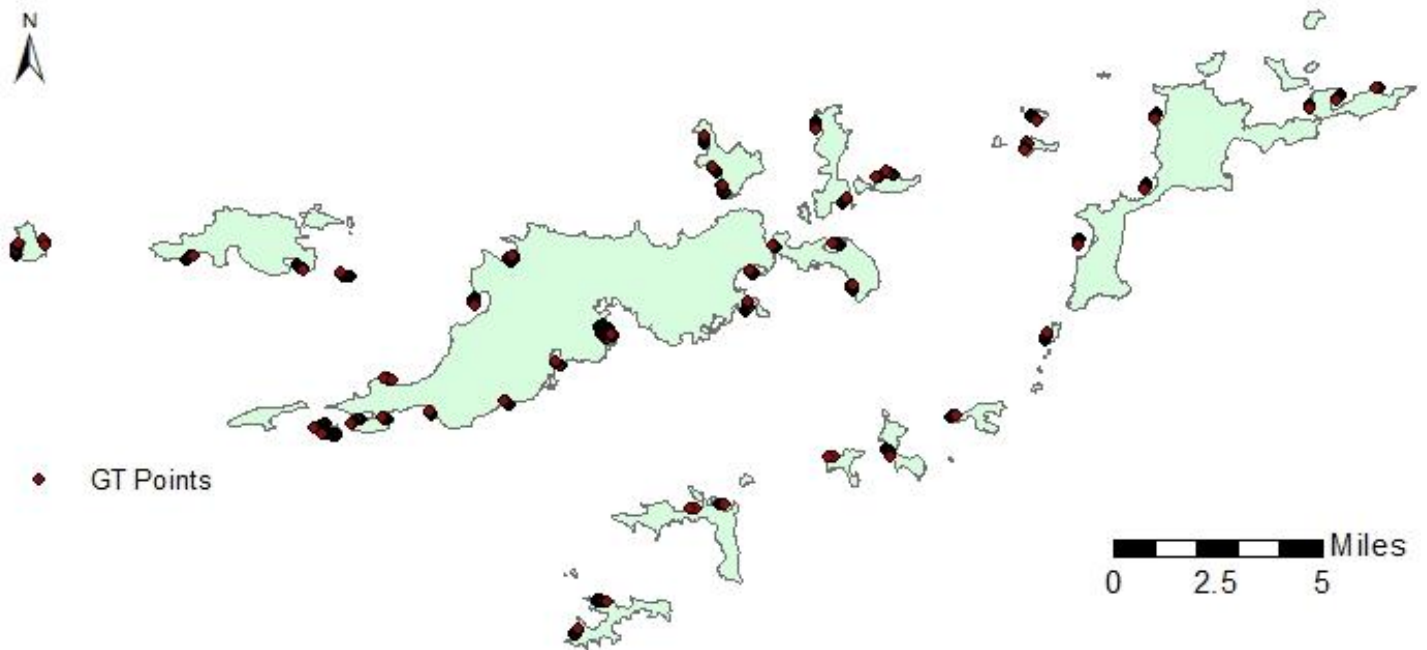


Figure 6: Location of ground-truth depth and habitat cover surveys conducted in June 2019.

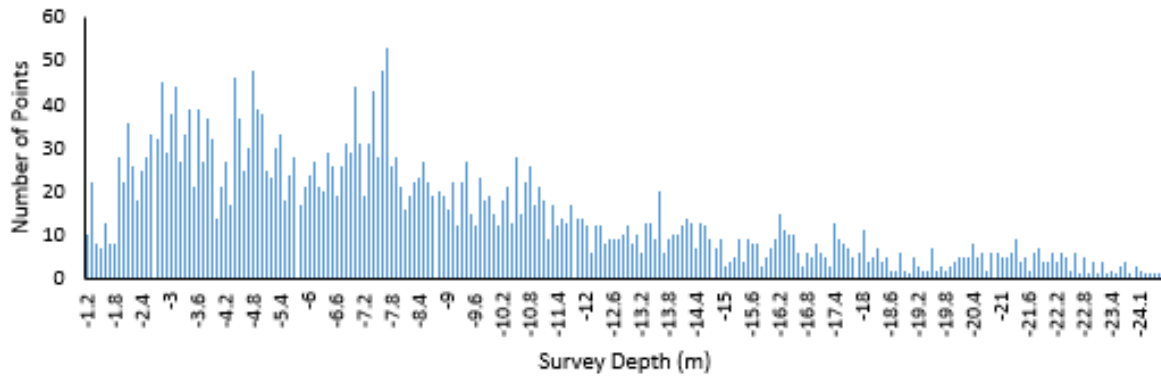


Figure 7: Count of post-Irma ground-truth survey training points for each depth.

Ground-Truth Data Collection

Sampling Strategy

Initial ground-truthing site selection was conducted by modelling Hurricane Irma impacts using ArcGIS. The model was constructed using data obtained from USGS-SRTM, CEFAS land cover, ReefBase, GEBCO and NOAA National Hurricane Centre. The maps produced were used to guide the selection of ground-truthing points in order to target worst-affected areas to assess the extent of the damage. The model and outcomes are presented in Appendix B. Final survey sites were selected based on the initial model and the local knowledge of the BVI National Parks Trust staff. Sites were spread over the entire archipelago, with the exception of Anegada, as rough weather prevented this excursion. Site selection depended heavily on access to the shallow water areas, as the presence of reefs often prevented this. Wherever possible, both leeward and windward sides of islands were sampled.

Field Measurements

Depth and GPS measurements were collected using a Deeper Sonar Pro+ device towed alongside the boat at a low speed (below 2 mph). Each transect was at least 50m in length and this was repeated at 42 sites of various depths (Figure 6). All sites were shallower than 25m, as SDB is inaccurate after this depth (Stumpf *et al.*, 2003).

Five sites were randomly selected along each transect and a GoPro Hero 4 camera was lowered on a weighted frame to approximately 50 cm from the seafloor. Photographs were taken every 10 seconds and the camera remained close to the seafloor for at least 90 seconds as the boat drifted. GPS coordinates were recorded using a Garmin handheld GPS every 10 seconds to correspond with the photographs. A total of 1643 suitable images were classified. Benthic habitat cover was determined by classifying 25 overlaid points to habitat type or species level in Coral Point Count (CPCe) software (Kohler and Gill, 2006; Phinn *et al.*, 2008). Each ground-truth image was classified according to the

classification scheme outlined in Figure 8. This classification scheme was adapted from Mumby and Harborne (1999); Fauzan *et al.* (2017); Manessa *et al.* (2014) and Wicaksono *et al.* (2019). The classes described are distinct enough to ensure the dominant class cover is associated with the reflectance value of that image object.

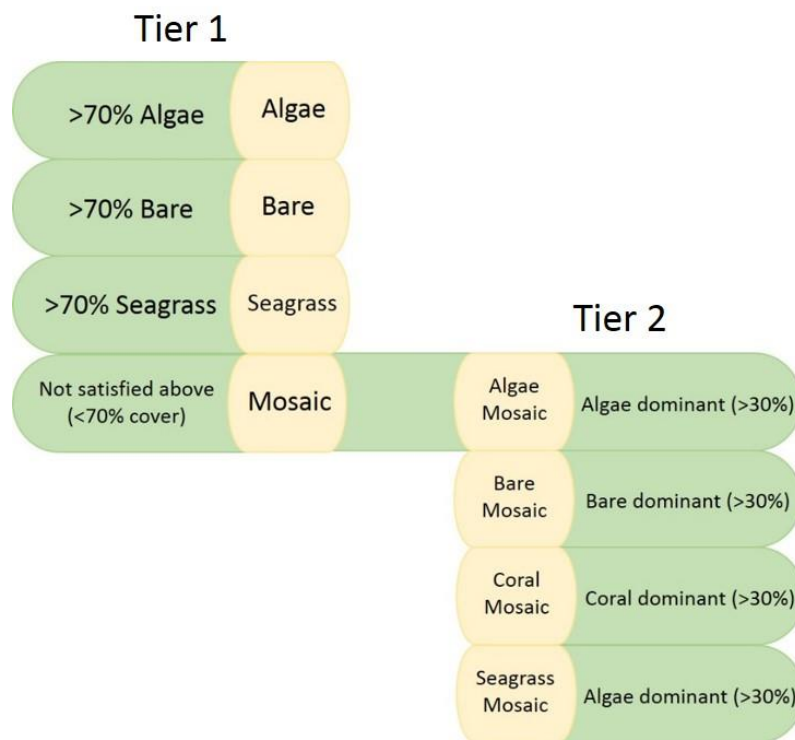


Figure 8: Classification scheme used to categorise benthic habitat images in CPCe. These classes give distinct spectral signatures to accurately train the segmented satellite images

Image Pre-Processing

SDB requires extensive pre-processing to eliminate the atmosphere and water column effects on spectral reflectance values. Image pre-processing was carried out using ENVI 5.0 software and ArcGIS. Each image was calibrated and processed separately to minimise errors (Caballero and Stumpf, 2019). Methods were finalised by adapting similar processing stages outlined in the literature (Hedley *et al.*, 2005; Hochberg *et al.*, 2003; Lyzenga, 1978; 1981; Mumby *et al.*, 1998; Phinn *et al.*, 2008; Stumpf *et al.*, 2003). Pre-processing steps are outlined below and in Figure 9.

1) Radiometric Calibration

Raw WorldView-2 images are already radiometrically corrected but require radiometric calibration to convert the pixel value from Digital Number (DN) to top-of-atmosphere reflectance using sensor-specific gain and offset values.

2) Orthorectification

Images were orthorectified against the USGS Shuttle Radar Topography Mission Digital Elevation Model and georeferenced in ArcGIS using ground-control points.

3) Land/Cloud/Shadow Masking

Areas of land, cloud and shadow were masked using a BVI land shapefile and manually-drawn cloud “Region of Interest” files.

4) Sunlint Correction

The masked images were then corrected for the effect of sunlint, which can distort the pixel values (Hedley *et al.*, 2005). The method outlined by Hochberg *et al.* (2003) and developed by Hedley *et al.* (2005) was followed to remove sunlint using the NIR band and Equation 1:

[Equation 1]

$$R'_i = R_i - b_i(R_{NIR} - Min_{NIR})$$

where R_i = radiance of band

b_i = regression slope of band i (y axis) against NIR band (x axis)

R_{NIR} = NIR radiance

Min_{NIR} = minimum NIR value

5) Convolution Filtering

A Low-Pass Filter with a 3x3 kernel size was applied to the glint-corrected images to reduce noise and smooth the image. Low pass filters reduce the discrepancy between pixel values by averaging adjacent pixel values.

6) Depth Invariant Index

Benthic habitat mapping requires the creation of a Depth Invariant Index (DII) image to correct for light attenuation through the water column (Mumby *et al.*, 1998). DII images were produced using the method developed by Lyzenga (1978; 1981) which requires linearised pixel values and applies a ratio of attenuation coefficients to each image, resulting in three DII files: Blue:Green, Blue:Red and Green:Red. The attenuation coefficients for pairs of spectral bands are determined using Equations 2 and 3:

[Equation 2]

$$slope = a + \sqrt{a^2 + 1}$$

Where $a = s_i^2 - s_j^2 / 2s_{ij}^2$

Where s^2 =variance of band and s_{ij}^2 = covariance between bands

[/Equation 3]

$$DII = \ln(R_i) - slope(\ln(R_j))$$

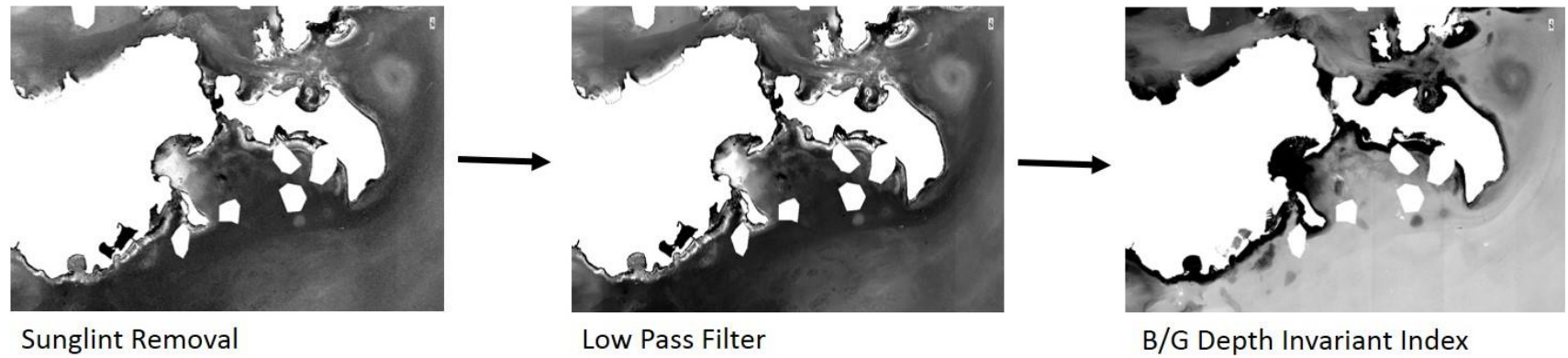
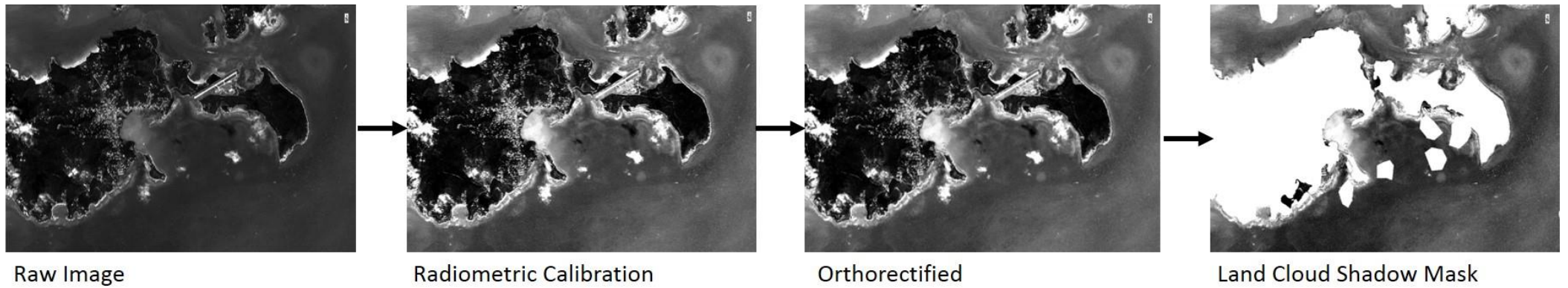


Figure 9: Image pre-processing stages correcting for radiometric and geometric distortion, sunglint and water column effects.

Bathymetry Derivation

Bathymetry was calculated using the empirical ratio transform approach outlined by Stumpf *et al.* (2003). This method utilises the ratio between two spectral bands to derive depth. The reflectance of the band with higher absorption will decrease proportionately faster than the band with lower absorption, meaning the ratio between the two will increase with depth (Stumpf *et al.*, 2003). The ratio transform method is more stable than previous linear transform methods, can retrieve depths over 25m and is not sensitive to variable substrate type, as changes in albedo affect both bands relatively equally (Stumpf *et al.*, 2003). The blue:green ratio gives the most reliable results compared to other band combinations (Stumpf *et al.*, 2003).

Depth measurements are calculated using equation 4:

[Equation 4]

$$z = m_1 \left(\frac{\ln(R_i)}{\ln(R_j)} \right) - m_0$$

where z = Absolute depth

$\ln(R_{i/j})$ = Linearised pixel value of band i/j

m_1 = slope of regression

m_0 = y intercept of regression

The blue:green ratio was applied to the pre-processed images to give single-banded images with pixel values of relative depth. The images were then trained using ground-truthing data. Extracted pixel values were regressed against absolute depth measurements to acquire the slope and y-intercept parameters. Equation 4 was applied to the reference images holding most ground-truth data points to obtain absolute depth values for each pixel. In the pre-Irma scene the reference image was used to train all other images. Absolute depth values extracted from the reference image formed new ground-truthing data to regress against pixel values of overlapping images. The ground-truth data collected for the post-Irma scene gave depth data across the entire BVI, so each image was trained separately. Final bathymetry maps were produced using ArcGIS. An extinction depth of 20m was selected, as this is commonly cited as the limit for accurate SDB depth retrieval (Stumpf *et al.*, 2003; Mumby *et al.*, 1998; Lyzenga, 1978; 1981) and the training scatter plot indicated an increase in variability beyond this depth.

Independent validation data points were used to extract SDB and absolute depth values from the ground-truth dataset. A linear regression was performed to provide estimates of Overall Accuracy, Mean Absolute Error and Root Mean Square Error.

Habitat Mapping

Benthic habitat determination was conducted using Trimble eCognition Developer 9.0 software. The reference images for each scene were segmented using the blue:green DII and the coastal and blue spectral bands of the de-glitched, filtered image. The strong penetration capacity of the coastal and blue bands makes them invaluable in defining benthic habitat extents (Lee *et al.*, 2013). Different segmentation parameters were trialled, and the final segmentation result was obtained using a scale parameter of 800, shape coefficient of 0.3 and a compactness coefficient of 1.0.

Image objects were classified using a Standard Nearest Neighbour algorithm trained with ground-truth benthic habitat data. The image object features that gave the best separation distance were used to assign classes. These were: mean brightness; mean B:G DII; mean B:R DII; mean G:R DII; mean blue; mean coastal; mean green; standard deviation B:G DII; standard deviation B:R DII; standard deviation G:R DII; standard deviation blue; standard deviation coastal; standard deviation green; max. difference. Figure 10 illustrates the overlap of reflectance values in a selection of bands between classes, which influences the classification accuracy. Seagrass classes are more distinctive in the pre-Irma scene and the variation in reflectance values of each class is higher in the post-Irma images (Figure 10).

All other images were segmented using the same parameters. The classification algorithms were applied to the P005 reference image of the pre-Irma scene and ground-truth samples were created from this classification image. Two other pre-Irma images were classified using ground-truth samples created in the overlapping area of P005. The overlap areas of the other images were not large enough to create ground-truth samples, so the pre-Irma scene does not include Virgin Gorda. The post-Irma ground-truth data covered the entire scene, so each image was classified separately using these data as samples. The classification images were then mosaicked together to create a single file for each scene.

Ground-truth habitat cover and modelled classification output values were extracted using validation data points. These data were used to create confusion matrices and calculate overall accuracy and kappa coefficients. Accuracy assessment using eCognition produced stability maps that illustrate the spatial distribution of errors.

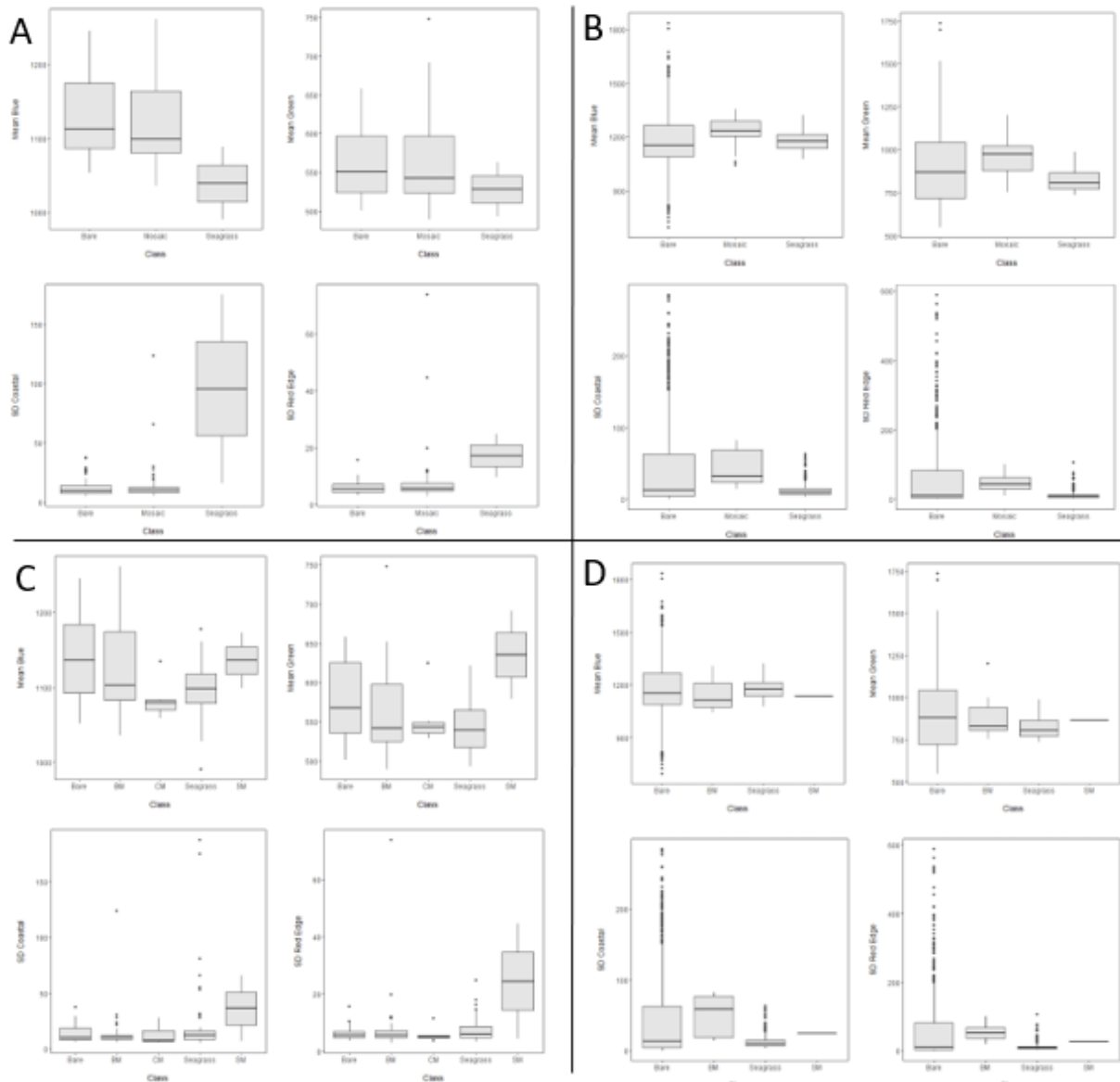


Figure 10: Class separation for Mean Blue, Mean Green, Standard Deviation Coastal and Standard Deviation Red Edge for (A) pre-Irma Tier 1; (B) post-Irma Tier 1; (C) pre-Irma Tier 2 and (D) post-Irma Tier 2.

Change Detection

Differences in bathymetry and habitat cover between the pre and post-Irma scenes were assessed using ArcGIS to produce a change image. The bathymetric change was then classified into meaningful thresholds according to the data to illustrate the spatial distribution and magnitude of depth changes in the BVI. Change thresholds must be outside the error margins to ensure the difference is significant. The habitat change map was classified into broad thresholds of “No Change” and “Change” but a more detailed map was also produced using the Tier 1 classification to show the nature of change.

Results

Bathymetry

The bathymetry detection provided detailed results with distinct differences shown between pixels. White areas close to shore represent bright shallow sand, which return erroneous positive depth values and are therefore misclassified as land.

The pre-Irma bathymetry map (Figure 11; 12) returned significantly more accurate results than the post-Irma bathymetry (Table 2). Validation plots show the pre-Irma bathymetry model explained 66% of the variation in MBES ground-truth depths whereas the post-Irma bathymetry model explained only 38% of the variation in survey depths (Figure 13; 14). There was considerably higher variation shown in the post-Irma validation depth points (Figure 14). The error associated with both pre and post-Irma bathymetry maps was low, with RMSE values of 2.42m and 3.84m and MAE of 0.078m and 0.44m respectively (Table 5). Initial exploration of the pre-Irma training data revealed separate relationships between SDB and MBES depths for vegetated and non-vegetated areas (Figure 15).

Significant positive change was shown to the south of Tortola and Virgin Gorda and around Norman and Peter Island, indicating these areas have become shallower (Figure 16). Areas to the north of Tortola and Virgin Gorda demonstrated negative change, meaning these areas have become deeper (Figure 16).

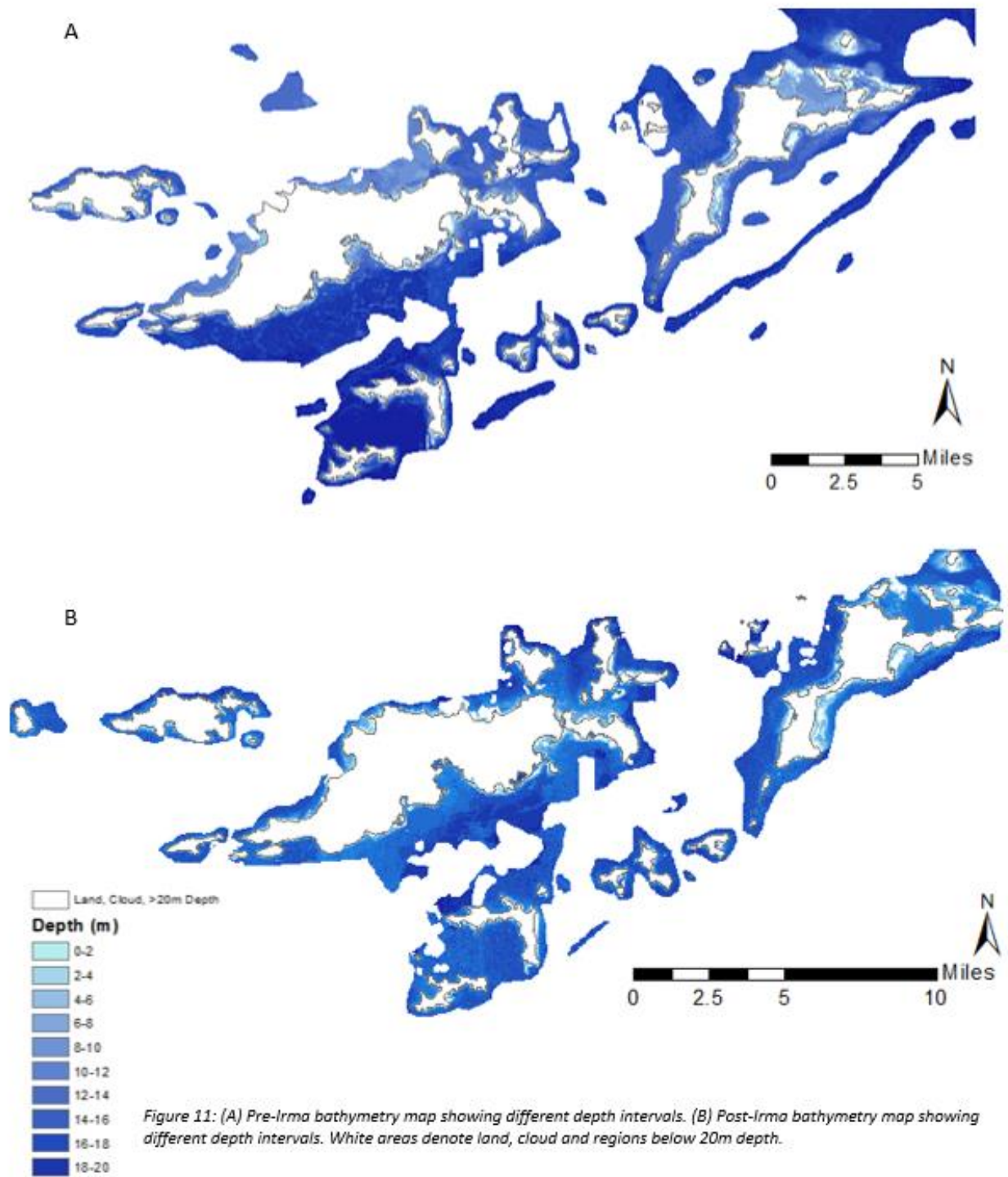


Figure 11: (A) Pre-Irma bathymetry map showing different depth intervals. (B) Post-Irma bathymetry map showing different depth intervals. White areas denote land, cloud and regions below 20m depth.

Figure 11: (A) Pre-Irma bathymetry map showing different depth intervals. (B) Post-Irma bathymetry map showing different depth intervals. White areas denote land, cloud and regions below 20m depth.

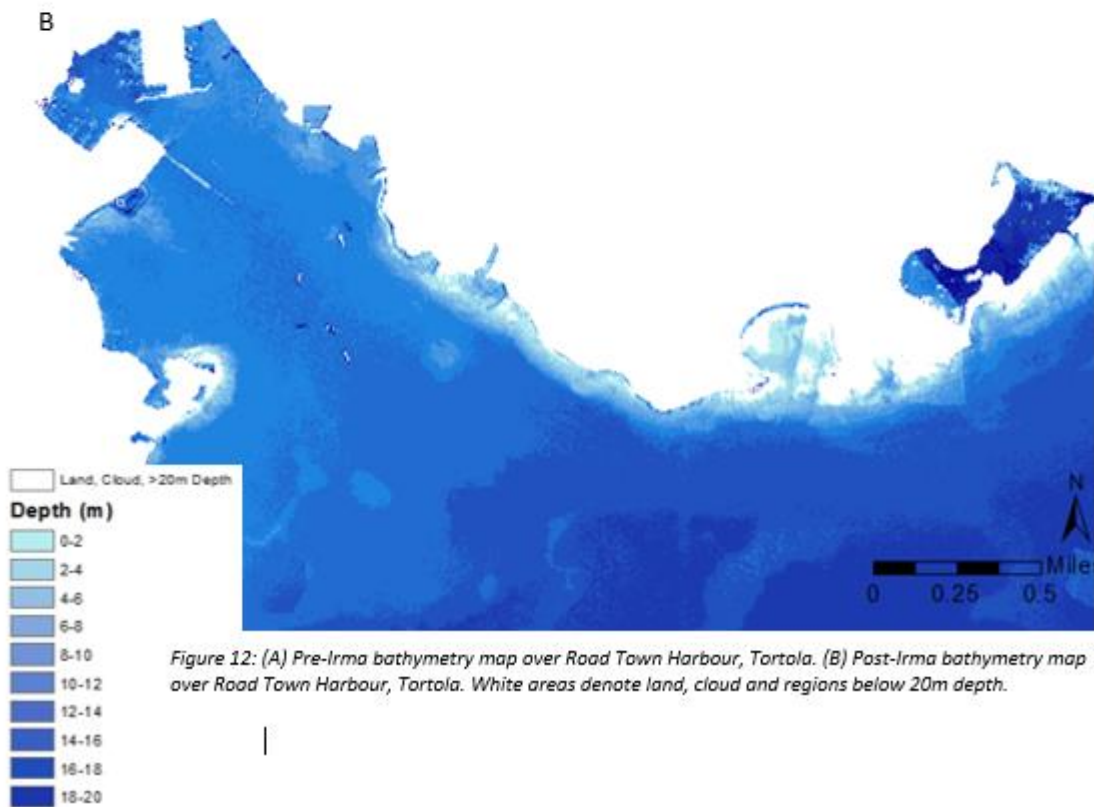
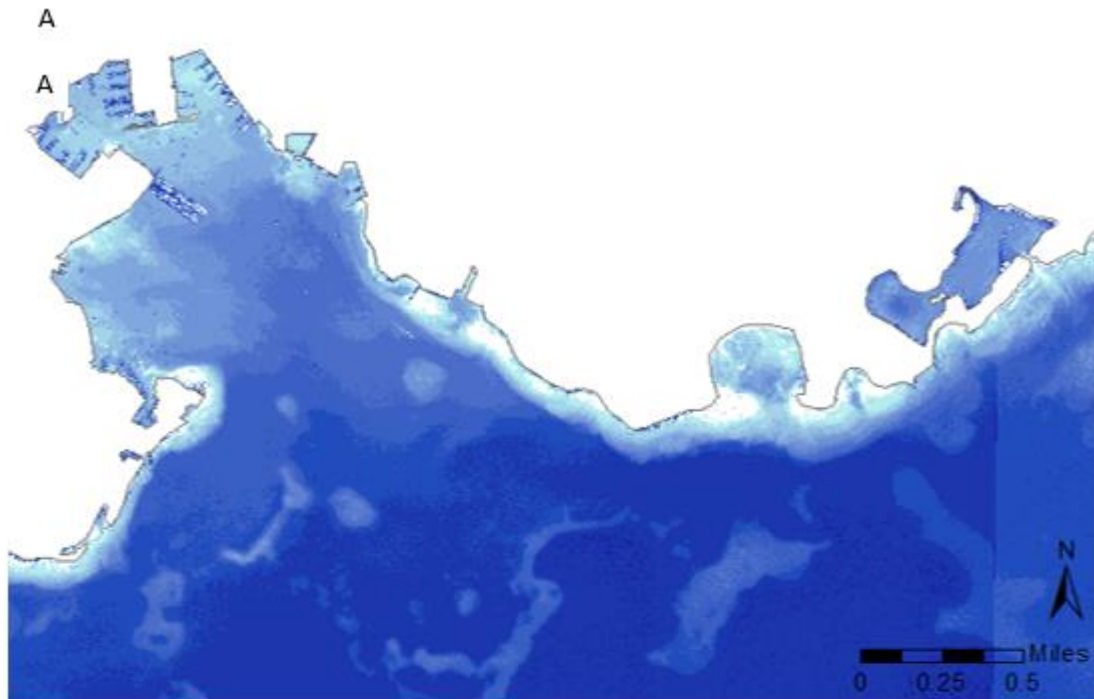


Figure 12: (A) Pre-Irma bathymetry map over Road Town Harbour, Tortola. (B) Post-Irma bathymetry map over Road Town Harbour, Tortola. White areas denote land, cloud and regions below 20m depth.

Figure 12: (A) Pre-Irma bathymetry map over Road Town Harbour, Tortola. (B) Post-Irma bathymetry map over Road Town Harbour, Tortola. White areas denote land, cloud and regions below 20m depth.

Table 2: Accuracy assessments of pre-Irma bathymetric map

	R ²	RMSE	MAE
Pre-Irma Bathymetry	0.6613	2.4215	0.0787
Post-Irma Bathymetry	0.3785	3.8399	0.4395

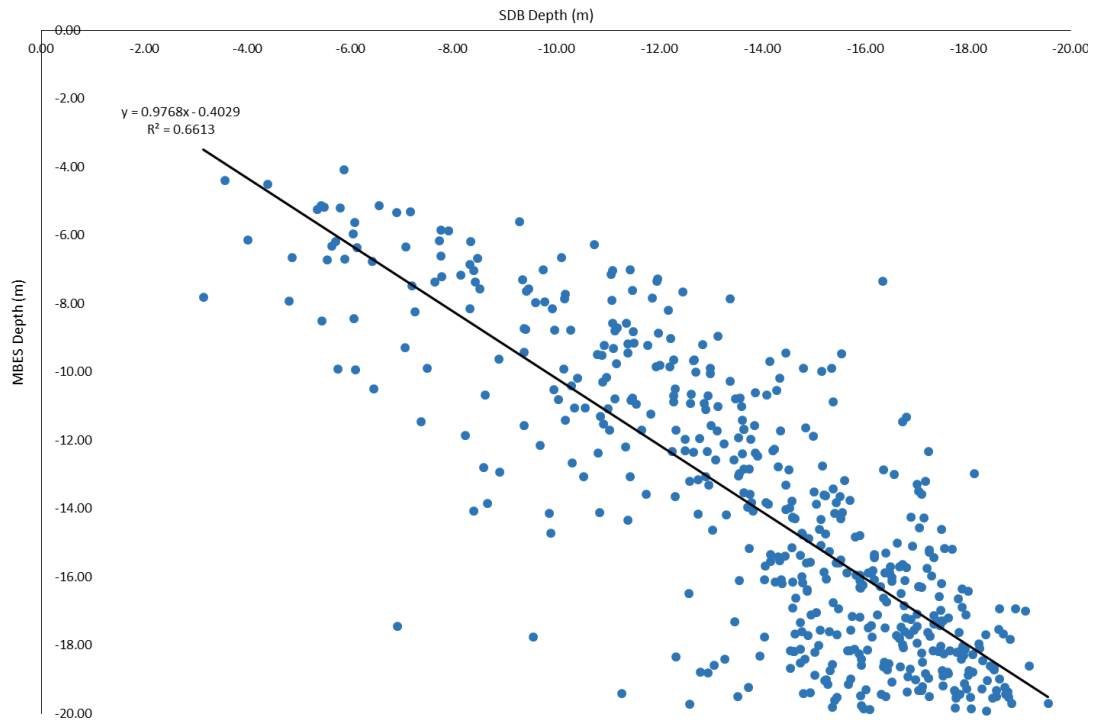


Figure 13: Validation plot of pre-Irma SDB depths against ground-truth MBES depth to an extinction depth of 20m.

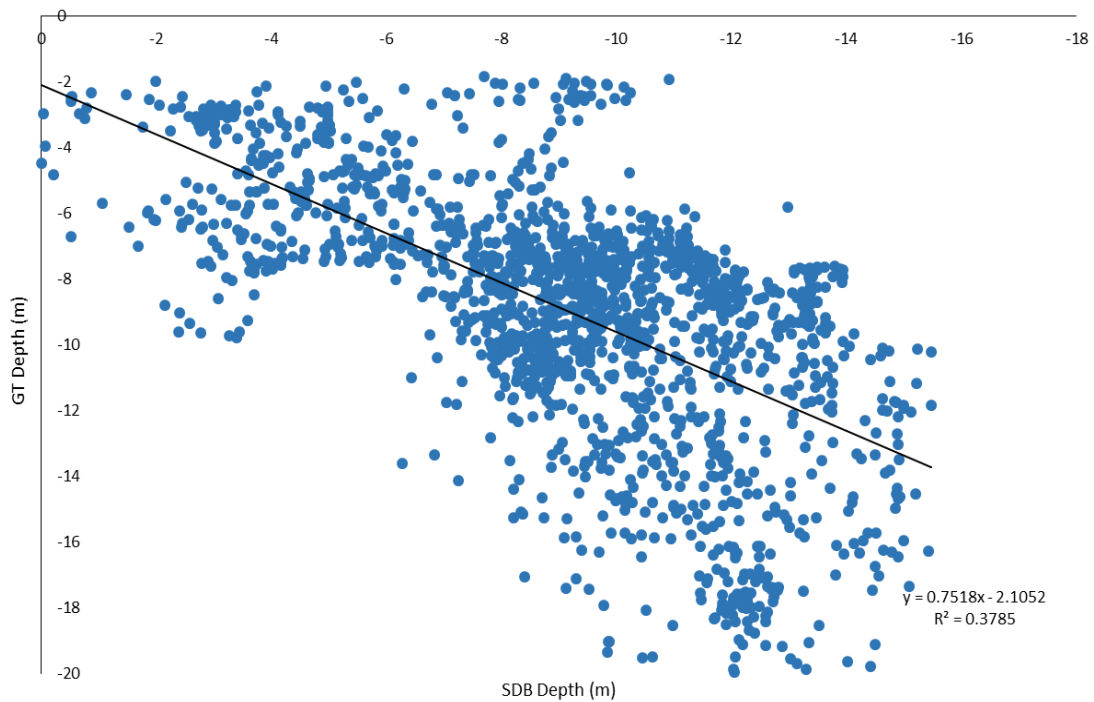


Figure 14: Validation plot for post-Irma SDB against survey ground-truth depth points with an extinction depth of 20m.

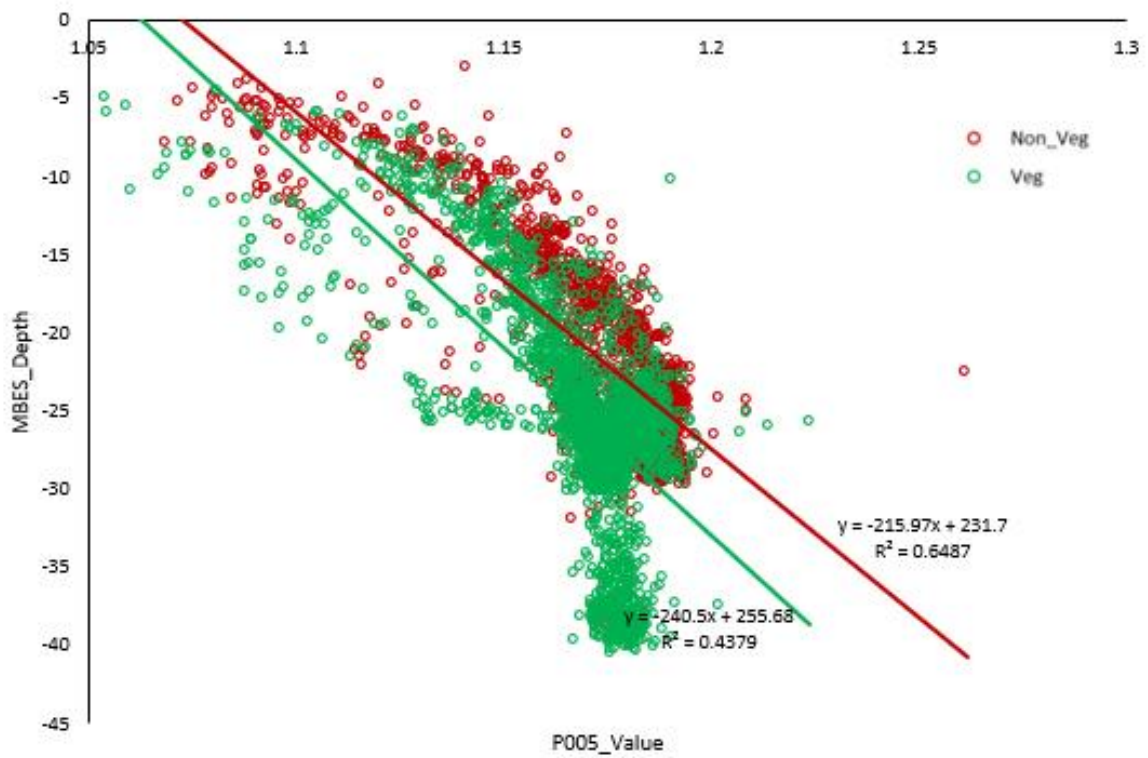


Figure 15: Training P005 to the MBES depth points with separate vegetated and non-vegetated areas. There appears to be different trends for each area, suggesting two different equations should be used to derive bathymetry.

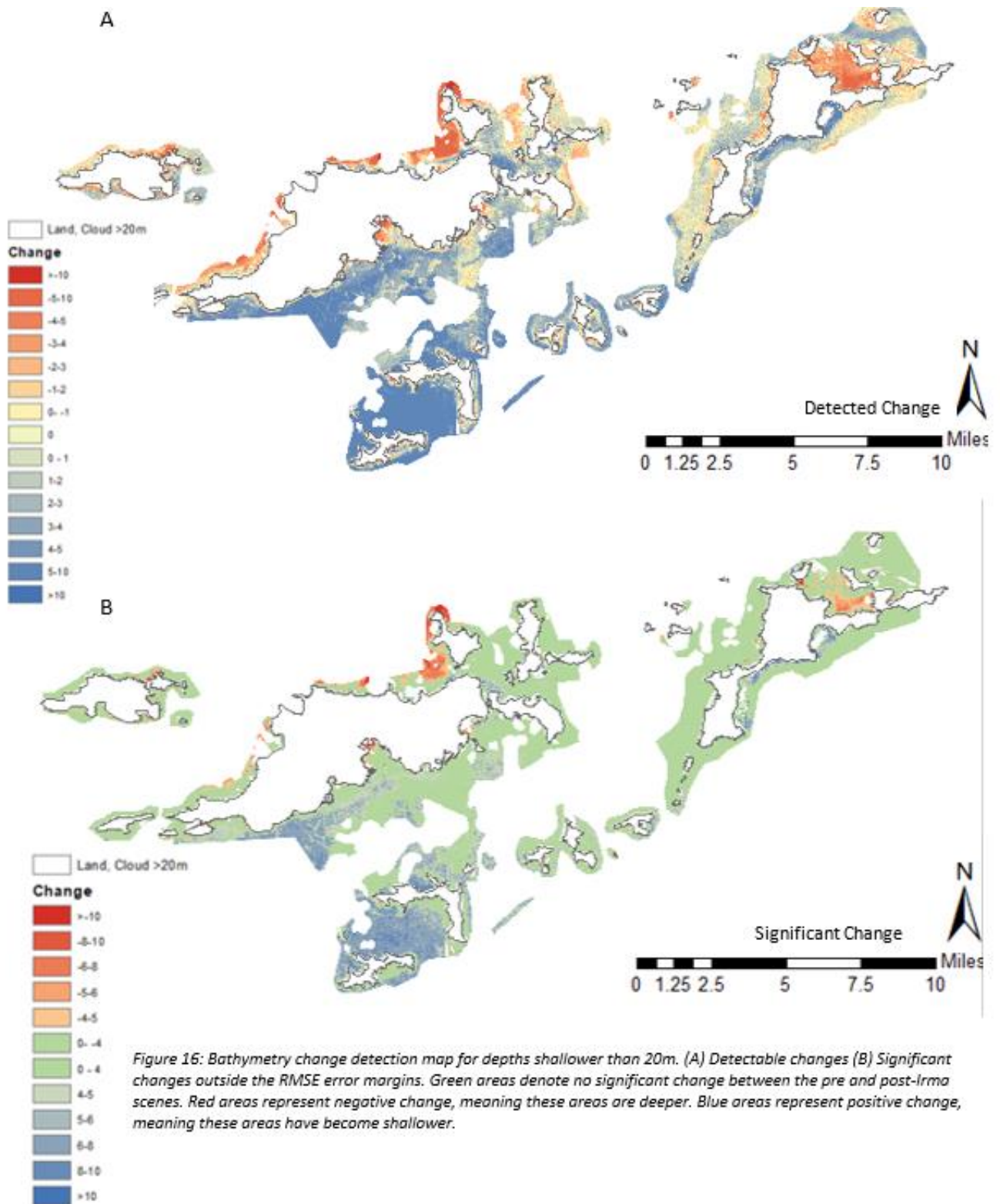


Figure 16: Bathymetry change detection map for depths shallower than 20m. (A) Detectable changes (B) Significant changes outside the RMSE error margins. Green areas denote no significant change between the pre and post-Irma scenes. Red areas represent negative change, meaning these areas are deeper. Blue areas represent positive change, meaning these areas have become shallower.

Figure 16: Bathymetry change detection map for depths shallower than 20m. (A) Detectable changes (B) Significant changes outside the RMSE error margins. Green areas denote no significant change between the pre and post-Irma scenes. Red areas represent negative change, meaning these areas are deeper. Blue areas represent positive change, meaning these areas have become shallower.

Habitat

Tier 1

Tier 1 maps yielded areas of Bare, Seagrass and Mosaic cover. There were not enough ground-truth algae samples to include this habitat in the classification process. The pre-Irma habitat map shows bare cover around Jost Van Dyke and northern Tortola while the area south of Tortola is classified as mosaic (Figure 17). The post-Irma map shows significantly more seagrass cover, completely surrounding the perimeter of Tortola and prevalent to the northeast of Virgin Gorda (Figure 17). Overall accuracy values of 62% and 67% were achieved for the pre-Irma and post-Irma Tier 1 habitat maps respectively (Tables 3; 4). The post-Irma map produced a higher kappa coefficient, indicating a stronger agreement between the modelled habitat classes and ground-truth data. The difference in user accuracies for each class illustrate the high variability in classifying different habitats.

Tier 2

Applying the Tier 2 classification scheme to the pre-Irma images returned areas of seagrass on the south side of Tortola and around Norman and Peter Island (Figure 18). Most bare areas in the Tier 1 map were found to be bare mosaic areas in the Tier 2 map. Some areas of Tier 1 mosaic were reclassified as bare cover, while others were categorised as coral and bare mosaic around Virgin Gorda (Figure 18). The pre-Irma Tier 2 map attained an overall accuracy of 51% while the post-Irma Tier 2 map was 65% accurate (Tables 5; 6). The post-Irma scene achieved a higher kappa coefficient, indicating a stronger agreement with the ground-truth samples (Tables 5; 6).

Figure 19 shows the change in habitat cover between the pre and post-Irma scenes. The majority of the area surrounding Jost Van Dyke showed no change, but an increase in seagrass cover was shown in the deeper areas. A marked increase in seagrass occurred to the south and southwest of Tortola, where bare and mosaic covers changed to seagrass (Figure 19). Increases in bare cover were evident in the deeper areas to the south of Tortola and the north of Peter Island, while the benthic cover around Norman Island remained relatively unchanged (Figure 19). Habitat changes show no relation to the Hurricane Irma track.

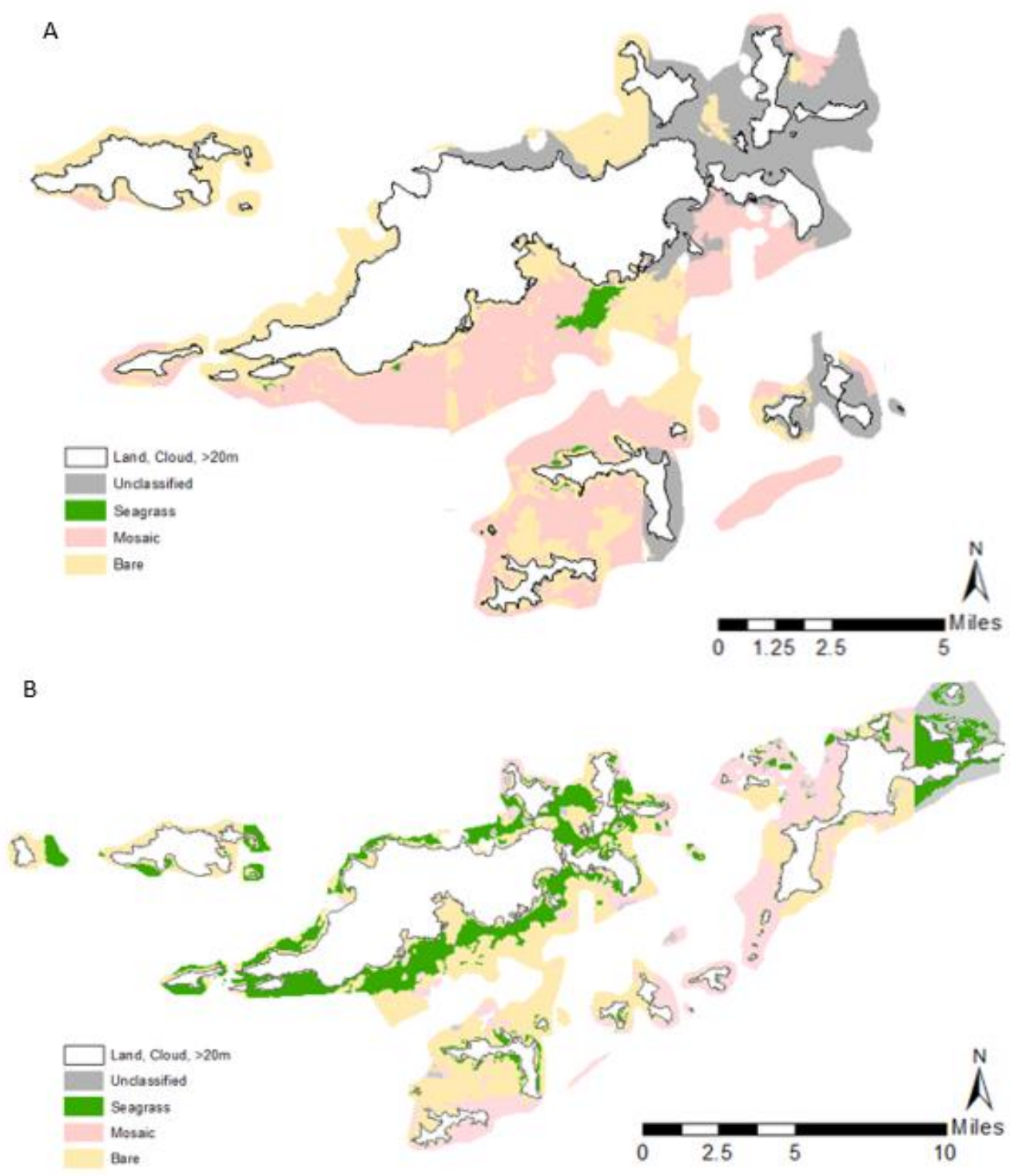


Figure 17: (A) Pre-Irma habitat Tier 1 classification (B) Post-Irma habitat Tier 1 classification

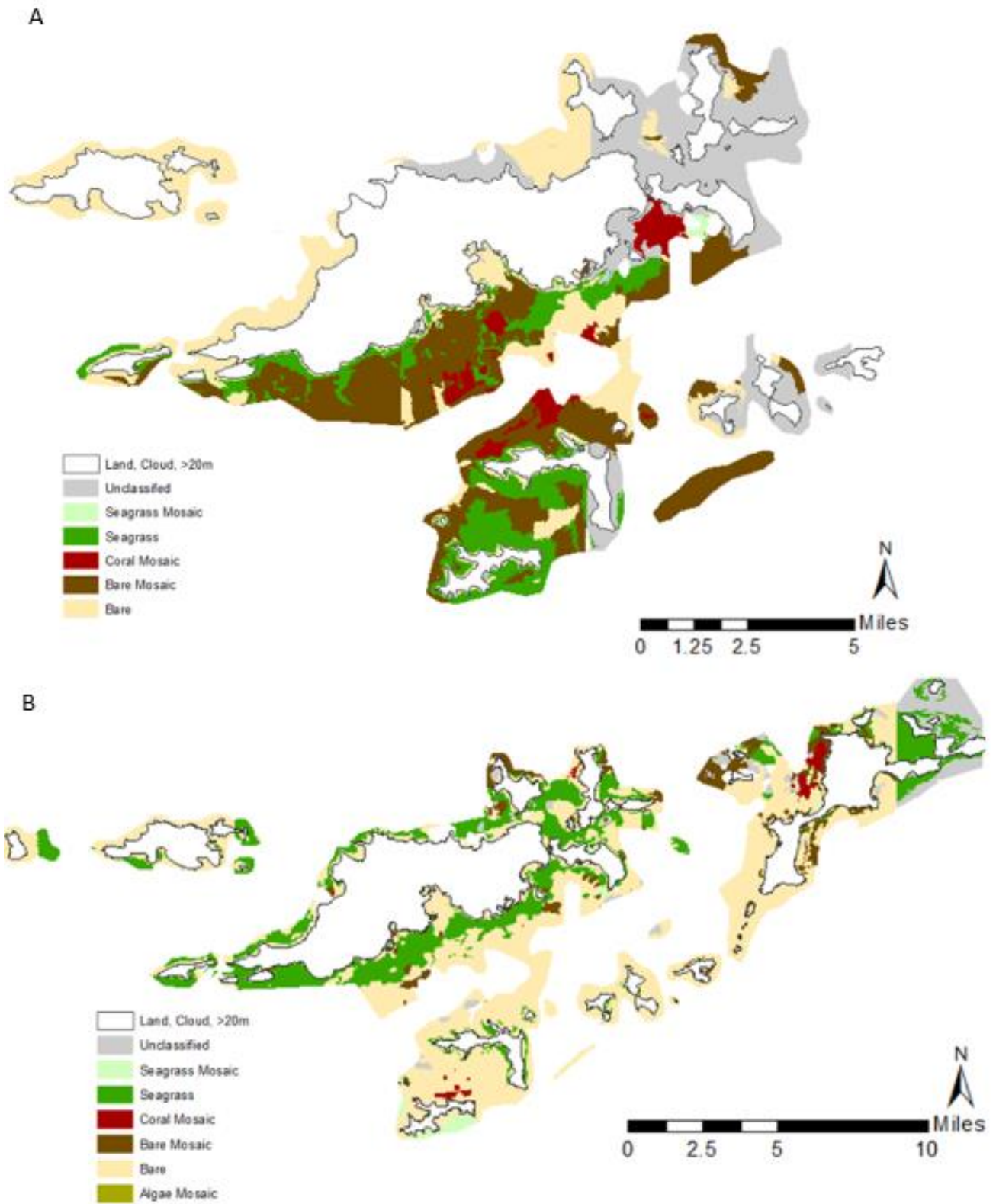


Figure 18: (A) Pre-Irma habitat Tier 2 classification (B) Post-Irma habitat Tier 2 classification

Table 3: Pre-Irma Tier 1 accuracy assessment

		Modelled Classes			
		Bare	Mosaic	Seagrass	Total
Ground Truth	Bare	23	8	0	31
	Mosaic	24	39	2	65
	Seagrass	1	3	1	5
	Total	48	50	3	101
Producer Accuracy		0.7419	0.6	0.2	
User Accuracy		0.4791	0.78	0.3333	
Overall Accuracy		0.6237			
Kappa Coefficient		0.2955			

Table 4: Post-Irma Tier 1 accuracy assessment.

		Modelled Classes						
		Algae	Bare	Coral	Mosaic	Seagrass	Unclass	Total
Ground Truth	Algae	0	1	0	0	0	0	1
	Bare	0	169	0	16	17	2	204
	Coral	0	1	0	3	0	0	4
	Mosaic	0	48	0	23	15	0	86
	Seagrass	0	26	0	0	68	0	94
	Total	0	245	0	42	100	2	389
Producer Accuracy		0	0.8284	0	0.2674	0.7234		
User Accuracy		0	0.6898	0	0.5476	0.68		
Overall Accuracy		0.6684						
Kappa Coefficient		0.4319						

Table 5: Pre-Irma Tier 2 accuracy assessment.

		Modelled Classes					
		Bare	BM	CM	Seagrass	SM	Total
Ground Truth	Bare	21	8	1	1	0	31
	BM	12	18	4	6	0	40
	CM	3	3	11	3	0	20
	Seagrass	1	1	1	1	1	5
	SM	0	1	3	0	1	5
	Total	37	31	20	11	2	101
Producer Accuracy		0.6774	0.45	0.55	0.2	0.2	
User Accuracy		0.5675	0.5806	0.55	0.0909	0.5	
Overall Accuracy		0.5148					
Kappa Coefficient		0.3265					

Table 6: Post-Irma Tier 2 accuracy assessment.

		Modelled Class									Total
		Algae	AM	Bare	BM	CM	Coral	Seagrass	SM	Unclass	
Ground Truth	Algae		0	1	0	0	0	0	0	0	1
	AM	0		3	2	0	0	0	0	0	5
	Bare	0	0		8	2	0	17	8	2	203
	BM	0	0	34		3	0	8	3	0	57
	CM	0	0	2	1		0	0	1	0	9
	Coral	0	0	1	0	3		0	0	0	4
	Seagrass	0	0	26	0	0	0		0	0	94
	SM	0	0	8	0	0	0	3		0	15
	Total	0	0	242	20	13	0	96	16	2	389
	Producer Accuracy	0	0	0.8177	0.1578	0.5556	0	0.7234	0.2667		
User Accuracy	0	0	0.6859	0.45	0.3846	0	0.7083	0.25			
Overall Accuracy	0.6478										
Kappa Coefficient	0.4186										

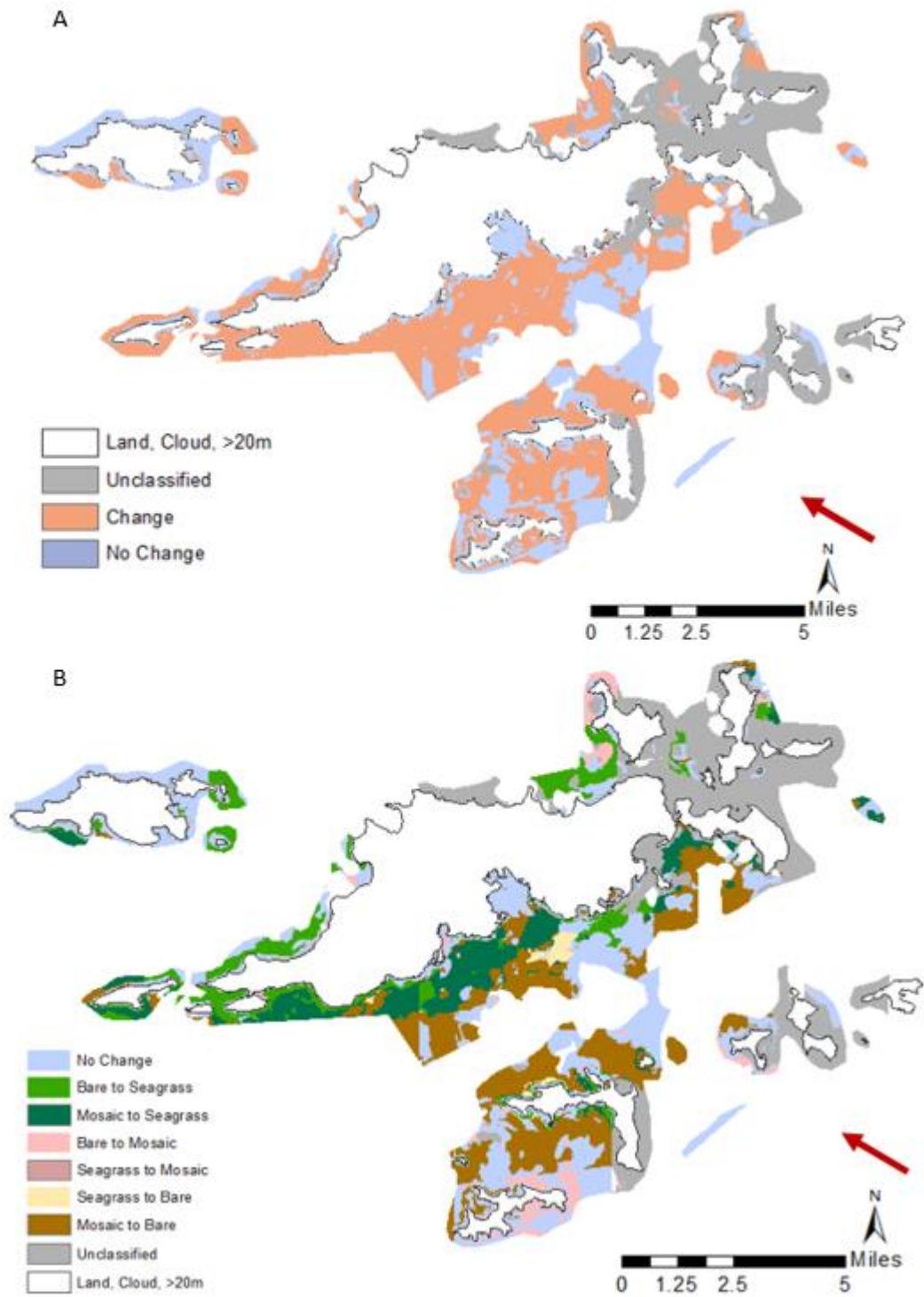


Figure 19: (A) Areas of habitat change following the 2017 Hurricane season; (B) Nature of habitat change following the Tier 1 habitat classification. The red arrow represents the path of Hurricane Irma.

Discussion

This research aimed to determine the bathymetry and benthic habitat cover of the BVI before and after Hurricane Irma and assess changes between the pre and post-Irma scenes. The outcomes of this study include detailed and accurate pre and post-Irma bathymetry and habitat cover maps (Figures 11; 12; 17; 18) that provide a baseline for future long-term monitoring schemes. The change detection analyses revealed areas of significant bathymetric and potential habitat change (Figures 16; 19). Modelled habitat changes are uncertain due to limited ground-truth data samples causing misclassification in the pre-Irma scene. This research feeds into work already completed by the Darwin Plus initiative in Anguilla and proposed work in the Turks and Caicos Islands. The project outputs can assist marine management in the BVI and have created a long-term monitoring framework for local researchers. Tracking changes in shallow-water ecosystems over a longer timescale will provide an insight into the impacts of climate change on marine environments.

Image Pre-Processing

Pre-processing visibly improved image clarity and minimised the effects of confounding factors. Masking the land, cloud and shadow areas proved to be a crucial step in image analysis, as this isolation of the areas of interest allowed a more accurate assessment of pixel values. The sunglint correction stage removed outliers caused by extreme pixel values and the application of the low pass filter significantly smoothed the image. Creating the Depth Invariant Index was also found to be an invaluable processing step, as these inputs increased the accuracy of image segmentation and classification.

Satellite Derived Bathymetry

The results demonstrate the success of SDB in estimating depth data for the BVI. Outputs illustrate fine-scale benthic features and show depth variations on a small spatial scale (Figures 11; 12). The higher accuracy of the pre-Irma bathymetry map (Table 2) highlights the strong relationship between the SDB values and MBES depths. The high variation in validation depths for the post-Irma scene (Figure 14) indicates a weaker relationship between the SDB model and absolute depths. The post-Irma ground-truth survey was conducted using a Deeper Sonar device designed for small-scale fish-finding whereas the pre-Irma ground-truth data was collected using a large-scale boat-mounted MBES device operated by CEFAS. This suggests the pre-Irma MBES depth data were more accurate and less prone to localised variations in sea conditions than the post-Irma survey data.

SDB depths were overestimated in coastal areas of bright, shallow sand, as some pixels returned values over 0. These bright areas of sand have been problematic in previous studies (Manessa *et al.*, 2014) and these incorrect values were removed from the final map. The results of this study fit within

the error margins of previous SDB studies. Lowest RMSE values reported are between 0.77m (Huang *et al.*, 2017) and 1.94m (Eugenio *et al.*, 2015) but higher values are common throughout the literature. Hernandez and Armstrong (2016) describe an RMSE of 3.16m and Pike *et al.*, 2019 report 8.99m for deeper regions. Caballero and Stumpf (2019) report MAE values of 0.5 and SDB estimates by Huang *et al.* (2017) show MAE values of 0.56-0.81m.

The success of SDB using WorldView-2 images supports the use of SDB techniques in future large-scale mapping studies. The high repeatability and accessibility of this method lends itself to time-series analysis and creates important research opportunities in the BVI, including the impact assessment of chronic stressors and discrete disturbance events, such as Hurricanes, on diverse shallow-water environments. The high spatial resolution and low cost of this research compared to MBES or LiDAR surveys consolidates SDB methods as an invaluable marine research tool.

Habitat Mapping

The habitat maps illustrate a high concentration of seagrass beds and fringing reefs in shallow coastal waters surrounding the BVI (Figure 18). The Tier 2 pre-Irma scene depicts a high abundance of coral mosaic and seagrass areas in the path of Hurricane Irma (Figure 18).

The Standard Nearest Neighbour algorithm classified the majority of image objects, but unclassified sections were returned in areas of very bright, shallow sand and deep areas, as the reflectance values of these benthic covers do not fit within calculated class thresholds. Habitat models were more accurate using the Tier 1 scheme, which reinforces the theory that broad classification schemes produce more robust results (Wicaksono *et al.*, 2019). The post-Irma scene achieved slightly higher overall accuracy values compared to the pre-Irma scene (Tables 3; 4; 5; 6). Previous studies report classification accuracy values ranging from 42% (Janowski *et al.*, 2018) to 98.86% (Mohamed *et al.*, 2018). The results of this study sit within the overall accuracy range of 55.85-77.66% achieved by OBIA (Siregar *et al.*, 2018). Accuracy values of this research could be increased by applying a more complex classification algorithm, such as Support Vector Machine.

The higher accuracy of the post-Irma scene is potentially due to the higher number of ground-truth samples in each class, as the pre-Irma scene was trained with only 101 data points compared to 389 in the post-Irma scene. Only five seagrass data points were present in the pre-Irma scene compared to 94 in the post-Irma scene. Areas of bare habitat cover were classified most accurately, followed by mosaic classes in Tier 1 (Tables 3; 4). Seagrass classification is inaccurate in the pre-Irma scene, with user accuracy values of between 9-30% compared to 68-71% in the post-Irma scene. The pre and post-Irma classification stability maps show significantly higher stability in bare and mosaic classes compared to seagrass areas (Appendix C).

Overlapping spectral values limits the accuracy of habitat classification. Seagrass samples were distinct in the blue, coastal and red edge bands of the pre-Irma scene, but are not easily separable in the post-Irma images due to the high variation in the data (Figure 10). Confusion matrices highlight the misclassification of bare and mosaic classes in all maps and of seagrass as bare classes, particularly in the post-Irma scene (Tables 3; 4; 5; 6). Coral mosaic classes were mischaracterised as bare mosaic areas due to overlapping spectral signatures (Figure 10). Fewer samples were misclassified in the post-Irma scene compared to the pre-Irma scene, emphasising the limitations of the pre-Irma ground-truth data.

Change Detection

Most depth changes in the BVI were within the RMSE margin of the bathymetry maps but areas of significant negative and positive change that were 4-6m outside the error margin were identified (Figure 16). Negative depth changes found to the north of Tortola and Virgin Gorda suggest the possible loss of reef habitats, removal of benthic cover and scouring of loose sediment often caused by Hurricanes (Alvarez-Filip *et al.*, 2011). Positive change to the south of the BVI is potentially the result of sediment deposition. Habitat changes indicate an increase in seagrass cover, particularly to the south of Tortola (Figure 19). Areas of mosaic habitat around Peter Island changed to bare cover, which suggests a loss in diversity in these areas. The unexpected increase in seagrass cover is most likely due to the low number of seagrass training samples in the pre-Irma scene compared to the post-Irma scene, as this resulted in the misclassification of seagrass areas to bare or mosaic classes in the pre-Irma map (Tables 3; 5). The spatial distribution of bathymetric and habitat changes was not related to the track of Hurricane Irma, as the impacts were felt throughout the BVI (Figure 19).

Limitations

Suspended sediment visible in the images could confound the bottom reflectance of the area and therefore influence the bathymetry and habitat predictions (Fauzan *et al.*, 2017; Koedsin *et al.*, 2016; Pike *et al.*, 2019).

While the pre-Irma MBES ground-truth data provides accurate depths at a high resolution, the data falls within one image only. All other images in the pre-Irma scene were trained to this reference image, which lowers the accuracy of the training process. There are also very few MBES values in shallow water areas, with the majority of the data points falling between 22-30m depth (Figure 5). This limits the training capacity of this data set, as the range of values is not representative of the shallow water environment. Many studies suggest SDB is inaccurate below 25m depth (Stumpf *et al.*, 2003), which means these depths in the MBES dataset are unsuitable for bathymetric training. The post-Irma ground-truth dataset holds significantly more points at shallower depths compared to the

MBES dataset (Figure 6), which could increase the accuracy of the post-Irma bathymetric training, as these data cover the target depth range of >25m more thoroughly. Classification of seagrass habitats was restricted by the low number of ground-truth samples in the pre-Irma dataset. More accurate classification results could be achieved with more evenly distributed training data.

Field survey data used to ground-truth the post-Irma scene was collected 21 months after the satellite images were acquired, which could lessen the suitability of these data to train the bathymetry and habitat models. Previous research states the field surveys should be conducted as close to the image acquisition date as possible (Halls and Costin, 2016).

Damage to shallow water ecosystems may not be detectable until up to two years after a disturbance event, as there are time lags in ecological responses (Meyer and Pu, 2012). Change detection analysis would benefit from acquiring satellite images from a range of dates before and after the disturbance event, as this would ensure changes were the result of that discrete event instead of natural, gradual changes.

Future Study

The accuracy of satellite imagery analysis could be increased by pan-sharpening the multispectral images with the high resolution panchromatic images acquired at the same time.

The variety of benthic habitats present in BVI mean a single equation to calculate bathymetry is insufficient (Halls and Costin, 2016). Previous research has found that habitats show different relationships between reflectance values and LiDAR depths (Halls and Costin, 2016). The presence of seagrass influences the relationship between water reflectance and depth, reducing the accuracy of SDB generation in these areas (Doxani *et al.*, 2012). Images could be subset by habitat type using masking techniques and separate SDB algorithms could be applied to increase accuracy (Halls and Costin, 2016; Doxani *et al.*, 2012). Initial training plots of the pre-Irma reference image suggested there were several patterns in the data that were unexplored. Linear regression of SDB and MBES depth values over different habitats indicated different trends for vegetated and non-vegetated areas (Figure 15). Unsupervised K-means classification was carried out on the pre-processed reference image and 30 classes were visually assessed and combined to form vegetated and non-vegetated classes. These classes were converted to vectors and used to create a vegetation mask. This section of the research was not completed due to time and data constraints. The limited spatial extent of the pre-Irma ground-truth data and the small image overlap of the pre-Irma scene does not yield enough data points over vegetated and non-vegetated habitats to provide robust training data for SDB. Future research with improved ground-truth data coverage could explore using different training algorithms over vegetated and non-vegetated areas.

Some papers advocate the separation of shallow and deep areas in habitat classification. Using the sunglint-corrected image as the classification input for shallow areas and the DII as the input for deep areas significantly increased the classification accuracy (Hafizt *et al.*, 2017).

The use of Principal Components Analysis or Min Noise Fraction transforms extracts reliable information and reduces noise and redundancy within the data (Marcello *et al.*, 2018). PCA reduces the number of dimensions but retains the original data of the first principle components, which provides clearer thematic maps (Marcello *et al.*, 2018). Future research could explore the application of these transformations to reduce noise.

Alternative methods of mosaicking satellite images could improve the cohesion between images to form a continuous scene. The Pseudo-Invariant Feature (PIF) approach involves regressing pixel values each band of two images against each other to generate coefficients (Schott *et al.*, 1988). Sample areas of bright and dark pixel values are selected, such as shallow sand and shallow seagrass habitats (Pike *et al.*, 2019). This approach corrects for differences in sensor responses, atmospheric conditions and illumination effects between acquisition times to create a seamless mosaic (Schott *et al.*, 1988; (Traganos *et al.*, 2018).

Conclusion

This research reinforces the application of satellite imagery analysis techniques to derive bathymetry and habitat cover for shallow-water marine environments. The accurate bathymetry maps generated provide crucial information to develop our understanding of the oceanographic processes underlying BVI marine ecosystems. Benthic cover maps and change detection analyses can be used to guide marine management efforts to effectively conserve biodiverse habitats. Remote sensing methods prove to be extremely cost-effective and accessible, creating exciting opportunities for future research. This study has produced valuable mapping outcomes for the BVI that provide baseline data for long-term ecological monitoring schemes. This original research is one of the first studies to assess Hurricane damage in shallow-water ecosystems using satellite imagery and the successful results highlight the great potential of this approach. The methods outlined establish a framework for assessing the impact of future disturbance events in the BVI and can be applied to similar settings worldwide. These applications of remote sensing techniques are particularly potent in light of accelerated climate change impacts on fragile marine ecosystems.

References

- Alvarez-Filip, L., Gill, J., Dulvy, N., Perry, A., Watkinson, A. and M. Côté, I. (2011). Drivers of region-wide declines in architectural complexity on Caribbean reefs. *Coral Reefs* 30: 1051-1060.
- Anggoro, A., Sumartono, E., Siregar, V., Agus, S., Purnama, D., Supriyono, S., Puspitosari, D., Listyorini, T., Sulisty, B. and Parwito, P. (2018). Comparing Object-based and Pixel-based Classifications for Benthic Habitats Mapping in Pari Islands. *Journal of Physics: Conference Series* 1114: 012049
- Bythell, J.C. (1997). Assessment of the impacts of hurricanes Marilyn and Luis and post-hurricane community dynamics at Buck Island Reef National Monument as part of the long-term coral reef monitoring program in the north-eastern Caribbean. Final Report US Department of Interior National Park Service.
- Bythell, J., Hillis-Starr, Z. M. and Rogers, C. (2000). Local variability but landscape stability in coral reef communities following repeated hurricane impacts. *Marine Ecology Progress Series* 204: 93-100.
- Caballero, I. and Stumpf, R. (2019). Retrieval of nearshore bathymetry from Sentinel-2A and 2B satellites in South Florida coastal waters. *Estuarine, Coastal and Shelf Science*. 226. 106277.
- Call, K.A., Hardy, J.D. and Wallin, D.O. (2003) Coral reef habitat discrimination using multivariate spectral analysis and satellite remote sensing, *International Journal of Remote Sensing*, 24:13, 2627-2639
- Cinner, J.E., Huchery, C., MacNeil, M.A. *et al.* (2016) Bright spots among the world's coral reefs. *Nature* 535 (7612): 416-419.
- Deidda, M. and Sanna, G. (2012). Bathymetric extraction using worldview-2 high resolution images. *International Archives of the Photogrammetry, Remote Sensing and Spatial Information Sciences* 39: 153-157.
- Doxani, G., Papadopoulou, M., Lafazani, P., Pikridas, C., & Tsakiri-Strati, M. (2012). Shallow-water bathymetry over variable bottom type using multispectral WorldView-2 Image. *International Archives of the Photogrammetry, Remote Sensing and Spatial Information Sciences*, Volume XXXIX-B8, 2012 XXII ISPRS Congress, 25 August – 01 September 2012, Melbourne, Australia.
- Eugenio, F., Marcello, J., Martin, J. (2015). High-Resolution Maps of Bathymetry and Benthic Habitats in Shallow-Water Environments Using Multispectral Remote Sensing Imagery. *IEEE Trans. Geosci. Remote Sens.* 53: 3539–3549.
- Evagorou, E. Mettas, C., Agapiou, A., Themistocleous, K., and Hadjimitsis, D. (2019). Bathymetric maps from multi-temporal analysis of Sentinel-2 data: The case study of Limassol, Cyprus. *Advances in Geosciences*. 45. 397-407.
- Fauzan, M.A., Kumara, I.S., Yogyantoro, R.N., Suwardana, S.W., Fadhilah, N.L., Nurmalasari, I., Apriyani, S., & Wicaksono, P. (2017). Assessing the Capability of Sentinel-2A Data for Mapping Seagrass Percent Cover in Jerowaru, East Lombok. *IJG* 49 (2): 85 – 93.
- Fitzsimmons C, Young S, Newman S, Stead SM, Polunin, NVC. (2016). Understanding and addressing the impact of threats to marine ecosystems in the UK Overseas Territories in the Caribbean. Final Report to Defra, March 2016
- Forster, J. et. al (2011) Marine Biodiversity in the Caribbean UK Overseas Territories: Perceived threats and constraints to environmental management. *Marine Policy* 35 (2011) 647-657.
- Gao, J. (2009). Bathymetric mapping by means of remote sensing: methods, accuracy and limitations. *Progress in Physical Geography* 33 (1): 103-116.
- Gardner, T., Côté, I. M., Gill, J., Grant, A. and Watkinson, A. (2003). Long-term Regional-wide declining in Caribbean corals. *Science* 301: 958-60.
- Gardner, T., Côté, I. M., Gill, J. A., Grant, A. and Watkinson, A. R. (2005). Hurricanes and Caribbean coral reefs: Impacts, recovery patterns and role in long-term decline. *Ecology* 86: 174-184.
- Hafizt, M., Manessa, M., Adi, N., Prayudha, B. (2017). Benthic Habitat Mapping by Combining Lyzenga's Optical Model and Relative Water Depth Model in Lintea Island, Southeast Sulawesi. *IOP Conference Series: Earth and Environmental Science*. 98: 012037
- Halls, J. and Costin, K. (2016). Submerged and Emergent Land Cover and Bathymetric Mapping of Estuarine Habitats Using WorldView-2 and LiDAR Imagery. *Remote Sensing* 8: 718.

- Hamylton, S.M., Hedley, J.D., & Beaman, R.J. (2015). Derivation of High-Resolution Bathymetry from Multispectral Satellite Imagery: A Comparison of Empirical and Optimisation Methods through Geographical Error Analysis. *Remote Sensing* 7: 16257-16273.
- Hedley, J.D, Harborne, A.R. and Mumby, P.J. (2005) Technical note: Simple and robust removal of sun glint for mapping shallow-water benthos, *International Journal of Remote Sensing* 26:10, 2107-2112.
- Hedley, J.D., Roelfsema, C., Brando, V., Giardino, C., Kutser, T., Phinn, S., Mumby, P.J., Barrilero, O., Laporte, J. and Koetz, B. (2018). Coral reef applications of Sentinel-2: Coverage, characteristics, bathymetry and benthic mapping with comparison to Landsat 8. *Remote Sensing of Environment* 216: 598-614.
- Hernandez, W. and Armstrong, R. (2016). Deriving Bathymetry from Multispectral Remote Sensing Data. *Journal of Marine Science and Engineering*. 4: 8.
- Hochberg, E.J., Atkinson, M.J., and Andréfouët, S. (2003). Spectral reflectance of coral reef bottom-types worldwide and implications for coral reef remote sensing. *Remote Sensing of Environment* 85: 159-173.
- Hoegh-Guldberg, O., Mumby, P.J., Hooten, A.J., Steneck, R.S., Greenfield, P., Gomez, E., Harvell, C.D., Sale, P.F., Edwards, A.J., & Caldeira, K. (2007). Coral reefs under rapid climate change and ocean acidification. *science*, 318, 1737-1742
- Huang, R., Yum K., Wang, Y., Wang, J., Mu, L. and Wang, W. (2017). Bathymetry of the Coral Reefs of Weizhou Island Based on Multispectral Satellite Images. *Remote Sensing* 9: 750.
- Hubbard, D., Parsons-Hubbard, K., Bythell, J. and Walker, N.D. (1991). The effects of Hurricane Hugo on the reefs and associated environments of St. Croix, US Virgin Islands - A preliminary assessment. *Journal of Coastal Research*. 8. 33-48.
- Hughes, T.P. (1994). Catastrophes, Phase Shifts, and Large-Scale Degradation of a Caribbean Coral Reef. *Science* 265: 1547-1551.
- Jagalingam, P., Akshaya, B.J. and Hegde, A.V. (2015). Bathymetry Mapping Using Landsat 8 Satellite Imagery. *Procedia Engineering* 116: 560-566.
- Klemas, V. V. (2009). The Role of Remote Sensing in Predicting and Determining Coastal Storm Impacts. *Journal of Coastal Research* 25: 1264-1275.
- Knutson, T.R., McBride, J.L., Chan, J., Emanuel, K., Holland, G., Landsea, C., Held, I., Kossin, J.P., Srivastava, A.K., and Sugi, M. (2010). Tropical cyclones and climate change. *Nature Geoscience* 3: 157-163.
- Koedsin, W., Intararuang, W., Ritchie, R., Huete, A. (2016). An Integrated Field and Remote Sensing Method for Mapping Seagrass Species, Cover, and Biomass in Southern Thailand. *Remote Sensing*. 8. 292.
- Kohler, K.E. and Gill, S.M. (2006). Coral Point Count with Excel extensions (CPCe): A Visual Basic program for the determination of coral and substrate coverage using random point count methodology. *Computers & Geosciences*, 32, 1259-1269.
- Lambin, E.F. and Strahlers, A.H. (1994) Change-vector analysis in multitemporal space: A tool to detect and categorize land-cover change processes using high temporal-resolution satellite data. *Remote Sensing of Environment* 48(2): 231-244.
- Lee, K., Olsen, R.C., Kruse, F.A., & Kim, A.M. (2013). Using multi-angle WorldView-2 imagery to determine bathymetry near Oahu, Hawaii. *Defense, Security, and Sensing*.
- Li, X., Yeh, A.G.O., 1998. Principal component analysis of stacked multi-temporal images for the monitoring of rapid urban expansion in the Pearl River Delta. *Int. J. Remote Sens.* 19 (8), 1501–1518.
- Lu, D., Mausel, P., Brondízio, E. and Moran, E. (2004). Change detection techniques. *International Journal of Remote Sensing* 25(12): 2365-2401.
- Lyzenga, D.R. (1978). Passive remote sensing techniques for mapping water depth and bottom features. *Appl. Opt.* 17: 379-383.

- Lyzenga, D.R. (1981). Remote sensing of bottom reflectance and water attenuation parameters in shallow water using aircraft and Landsat data. *Int. J. Remote Sens.* 1: 71-82.
- Lyzenga, D.R. (1985) Shallow-Water Bathymetry Using Combined Lidar and Passive Multispectral Scanner Data. *International Journal of Remote Sensing*, 6, 115-125.
- Manessa, M.D.M., Kanno, A., Sekine, M., Ampou, E.E., Widagti, N., As-syakur, A.R. (2014). Shallow-Water Benthic Identification Using Multispectral Satellite Imagery: Investigation on the Effects of Improving Noise Correction Method and Spectral Cover. *Remote Sens.* 6: 4454-4472.
- Mann, M.E. and Emanuel, K.A. (2006). Atlantic hurricane trends linked to climate change. *Eos Trans. AGU* 87: 233-241.
- Marcello, J., Eugenio, F., Martín, J., Marqués, F. (2018). Seabed Mapping in Coastal Shallow Waters Using High Resolution Multispectral and Hyperspectral Imagery. *Remote Sens.* 10: 1208.
- Meyer, C.A. and Pu, R. (2012). Seagrass resource assessment using remote sensing methods in St. Joseph Sound and Clearwater Harbor, Florida, USA. *Environ Monit Assess* 184: 1131-1143.
- Mohamed, H., Nadaoka, K., Nakamura, T. (2018). Assessment of Machine Learning Algorithms for Automatic Benthic Cover Monitoring and Mapping Using Towed Underwater Video Camera and High-Resolution Satellite Images. *Remote Sens.* 10: 773.
- Moniruzzaman, M., Islam, S., Lavery, P., Bennamoun, M., Lam, C. (2019). Imaging and Classification Techniques for Seagrass Mapping and Monitoring: A Comprehensive Survey.
- Mumby, P.J., Clark, C.D., Green, E.P., and Edwards, A.J. (1998). Benefits of water column correction and contextual editing for mapping coral reefs. *International Journal of Remote Sensing*, 19, 203-210.
- Mumby, P. (1999). Bleaching and hurricane disturbances to populations of coral recruits in Belize. *Marine Ecology Progress Series* 190: 27-35.
- Mumby, P.J., and Harborne, A.R. (1999). Development of a systematic classification scheme of marine habitats to facilitate regional management and mapping of Caribbean coral reefs. *Biological Conservation* 88: 155-163.
- Pe'eri, S., Parrish, C., Azuike, C., Alexander, L., Armstrong. (2014). Satellite Remote Sensing as a Reconnaissance Tool for Assessing Nautical Chart Adequacy and Completeness. *Marine Geodesy.* 37 (3).
- Phinn, S., Roelfsema, C., Dekker, A., Brando, V., & Anstee, J. (2008). Mapping seagrass species, cover and biomass in shallow waters: An assessment of satellite multi-spectral and airborne hyperspectral imaging systems in Moreton Bay (Australia). *Remote Sensing of Environment*, 112, 3413-3425.
- Pike, S., Traganos, D., Poursanidis, D., Williams, J., Medcalf, K., Reinartz, P., Chrysoulakis, N. (2019). Leveraging Commercial High-Resolution Multispectral Satellite and Multibeam Sonar Data to Estimate Bathymetry: The Case Study of the Caribbean Sea. *Remote Sens.* 11: 1830.
- Pu, R., Bell, S., Baggett, L., Meyer, C., and Zhao, Y. (2012) Discrimination of Seagrass Species and Cover Classes with in situ Hyperspectral Data. *Journal of Coastal Research* 28 (6): 1330 – 1344.
- Rogers, C.S. (2000). Is *Acropora palmata* (Elkhorn Coral) making a comeback in the Virgin Islands? *Reef Encounter* 27: 15-17.
- Schott, J.R, Salvaggio, C. and Volchok, W.J. (1988). Radiometric scene normalisation using Pseudoinvariant Features. *Remote Sensing of Environment* 26: 1-16.
- Short, F.T., Polidoro, B., Livingstone, S.R., Carpenter, K.E., Bandeira, S., Bujang, J.S., Calumpong, H.P., Carruthers, T.J.B., Coles, R.G., & Dennison, W.C. (2011). Extinction risk assessment of the world's seagrass species. *Biological conservation*, 144, 1961-1971.
- Siregar, V.P., Agus, S.B, Subarno, T. and Prabowo, N.W. (2018). Mapping shallow waters habitats using OBIA by applying several approaches of depth invariant index in North Kepulauan Seribu. *OP Conf. Ser.: Earth Environ. Sci.* 149 012052.
- Stumpf, R., Holderied, K. and Sinclair, M. (2003). Determination of Water Depth with High-Resolution Satellite Imagery over Variable Bottom Types. *Limnology and Oceanography* 48: 547-556.

- Topouzelis, K., Spondylidis, S., Papakonstantinou, A., Soulakellis, N. (2016). The use of Sentinel-2 imagery for seagrass mapping: Kalloni Gulf (Lesvos Island -Greece) case study.
- Traganos, D., Poursanidis, D., Aggarwal, B., Chrysoulakis, N., & Reinartz, P. (2018). Estimating Satellite-Derived Bathymetry (SDB) with the Google Earth Engine and Sentinel-2. *Remote Sensing*, 10, 859.
- Wicaksono, P., Aryaguna, P. A. and Wahyu, L. (2019). Benthic Habitat Mapping Model and Cross Validation Using Machine-Learning Classification Algorithms. *Remote Sensing*. 11. 1279.
- Wicaksono, P. (2016). Improving the accuracy of Multispectral-based benthic habitats mapping using image rotations: the application of Principle Component Analysis and Independent Component Analysis. *European Journal of Remote Sensing*. 49. 433-463.

Appendix A: Image Parameter Tables

Table 1: Pre-Irma WorldView-2 imagery details.

Image	No. Columns	No. Rows	Acquisition Time	Cloud Cover	Sun Azimuth	Sun Elevation
054689891010_01_P001_MUL	3570	23750	2013-02-13 15:24:53	0.1%	150.7°	54.3°
054689891010_01_P002_MUL	8678	31058	2013-12-09 15:12:08	0.3%	160.5°	46.4°
054689891010_01_P003_MUL	8733	31055	2013-12-09 15:12:01	0.4%	160.6°	46.4°
054689891010_01_P004_MUL	8751	23924	2013-12-09 15:24:59	0.5%	150.9°	54.3°
054689891010_01_P005_MUL	8788	31061	2013-12-09 15:12:33	1.6%	160.4°	46.3°
054689891010_01_P006_MUL	10128	31068	2014-12-24 14:56:37	2.0%	154.2°	43.8°

Image	No. Columns	No. Rows	Acquisition Time	Cloud Cover	Sun Azimuth	Sun Elevation
057338465050_01_P001_MUL	10997	8769	2017-09-24 15:19:45	5%	145.4°	67.3°
057338465050_01_P002_MUL	14759	9058	2017-09-24 15:20:43	7.7%	146.2°	67.5°
057338465050_01_P003_MUL	22889	12490	2017-09-10 15:35:44	16.1%	143.6°	73.4°
057338465050_01_P004_MUL	13271	8009	2017-09-28 14:31:56	29.4%	128.5°	58.6°
057338465050_01_P005_MUL	10779	8926	2017-09-24 15:17:53	4%	144.1°	67.0°

Table 2: Post-Irma WorldView-2 imagery details.

Table 3: Training and validation point coverage for each satellite image.

Image	No. Training Points	No. Validation Points
054689891010_01_P001_MUL	1897	1897
054689891010_01_P002_MUL	2063	2063
054689891010_01_P004_MUL	1989	1988
054689891010_01_P005_MUL	2048	1244
054689891010_01_P006_MUL	2148	2148
057338465050_01_P001_MUL	1701	1701
057338465050_01_P002_MUL	1282	1281
057338465050_01_P003_MUL	741	741
057338465050_01_P004_MUL	317	316
057338465050_01_P005_MUL	798	798

Appendix B: Preliminary Ground-Truth Site Selection

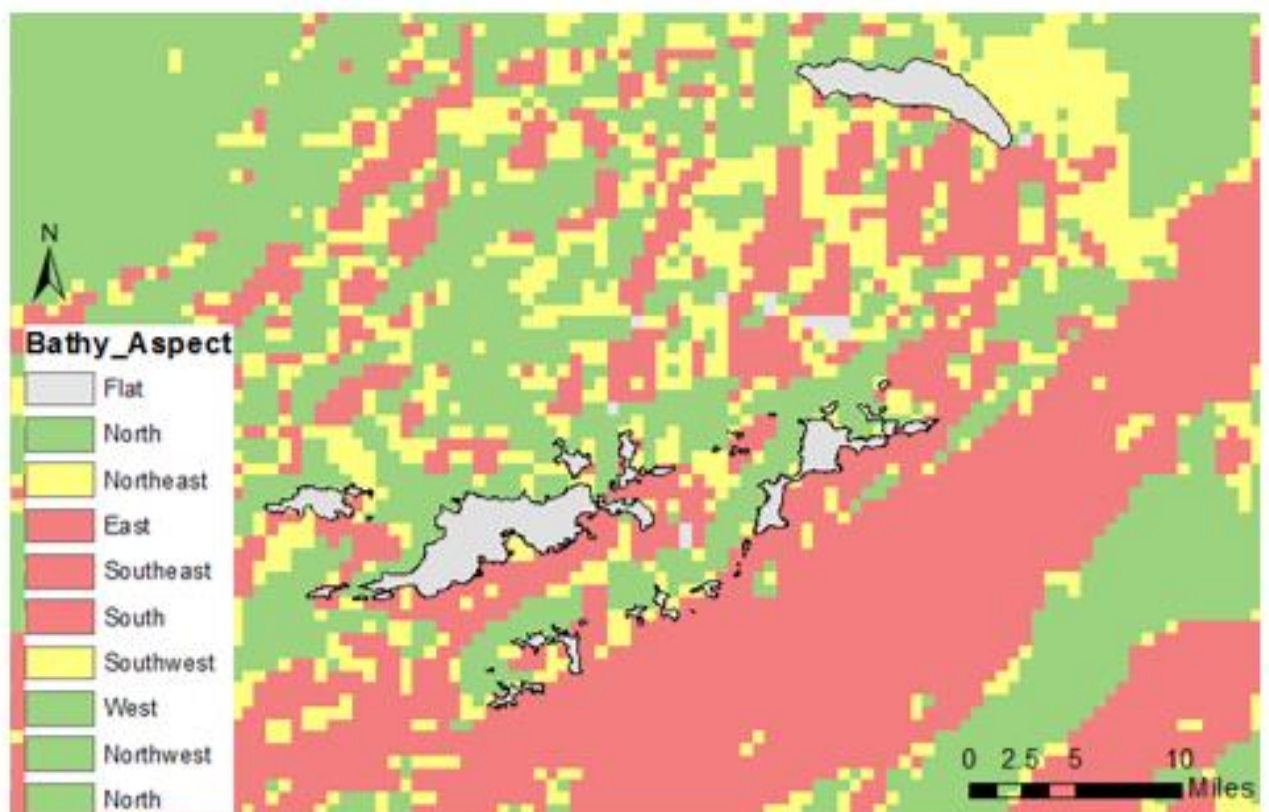


Figure B:1: Aspect of the bathymetry of the BVI with the most exposed areas (to the South, East and Southeast) highlighted in red.

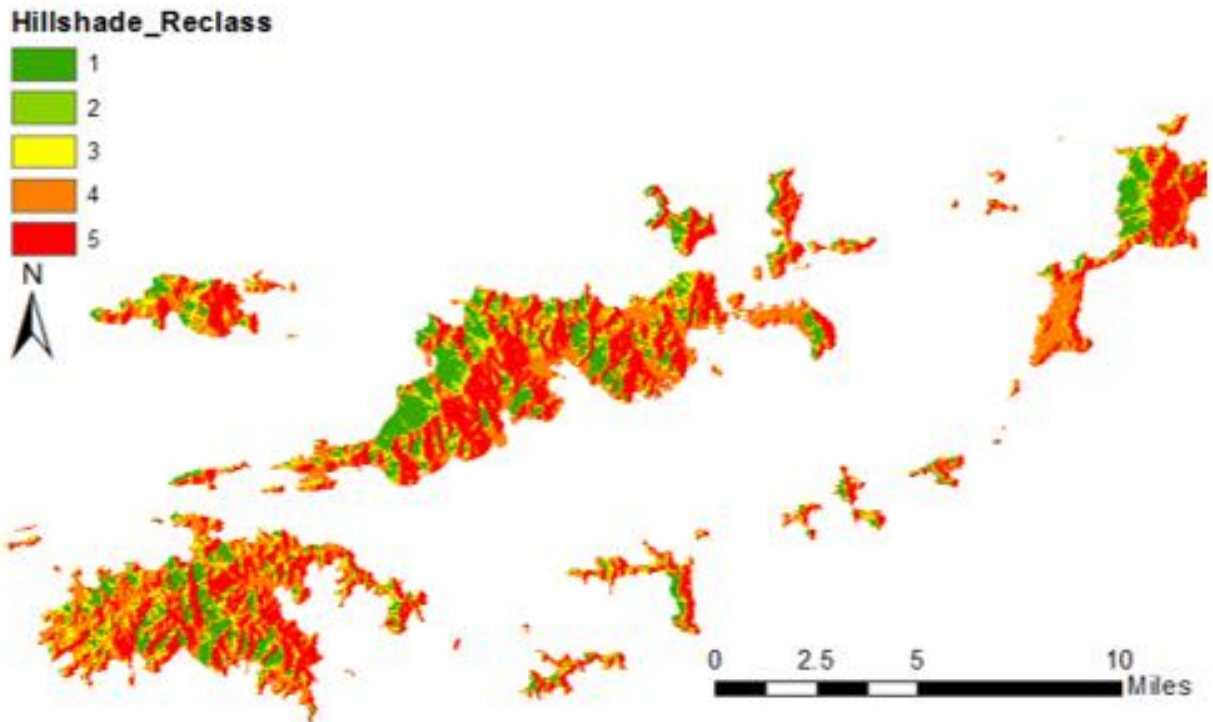


Figure B:2: The hillshade effect of the BVI classified into five ranks, with red representing the most exposed areas and green the sheltered areas. The south-east coastline of the islands was most exposed to Hurricane Irma.

Appendix C: Habitat Classification Stability

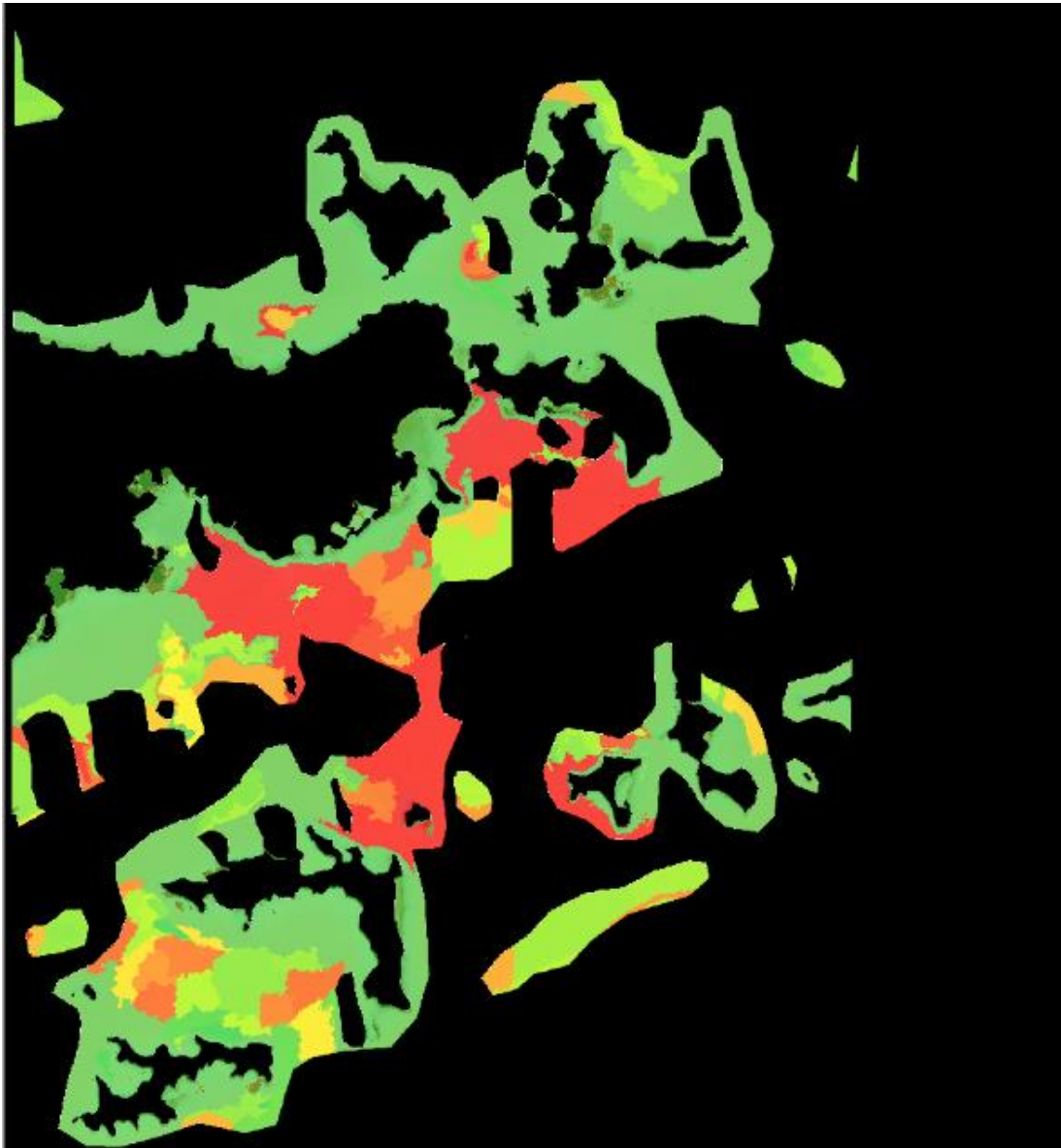


Figure C:1: Pre-Irma habitat classification stability for reference image P005.

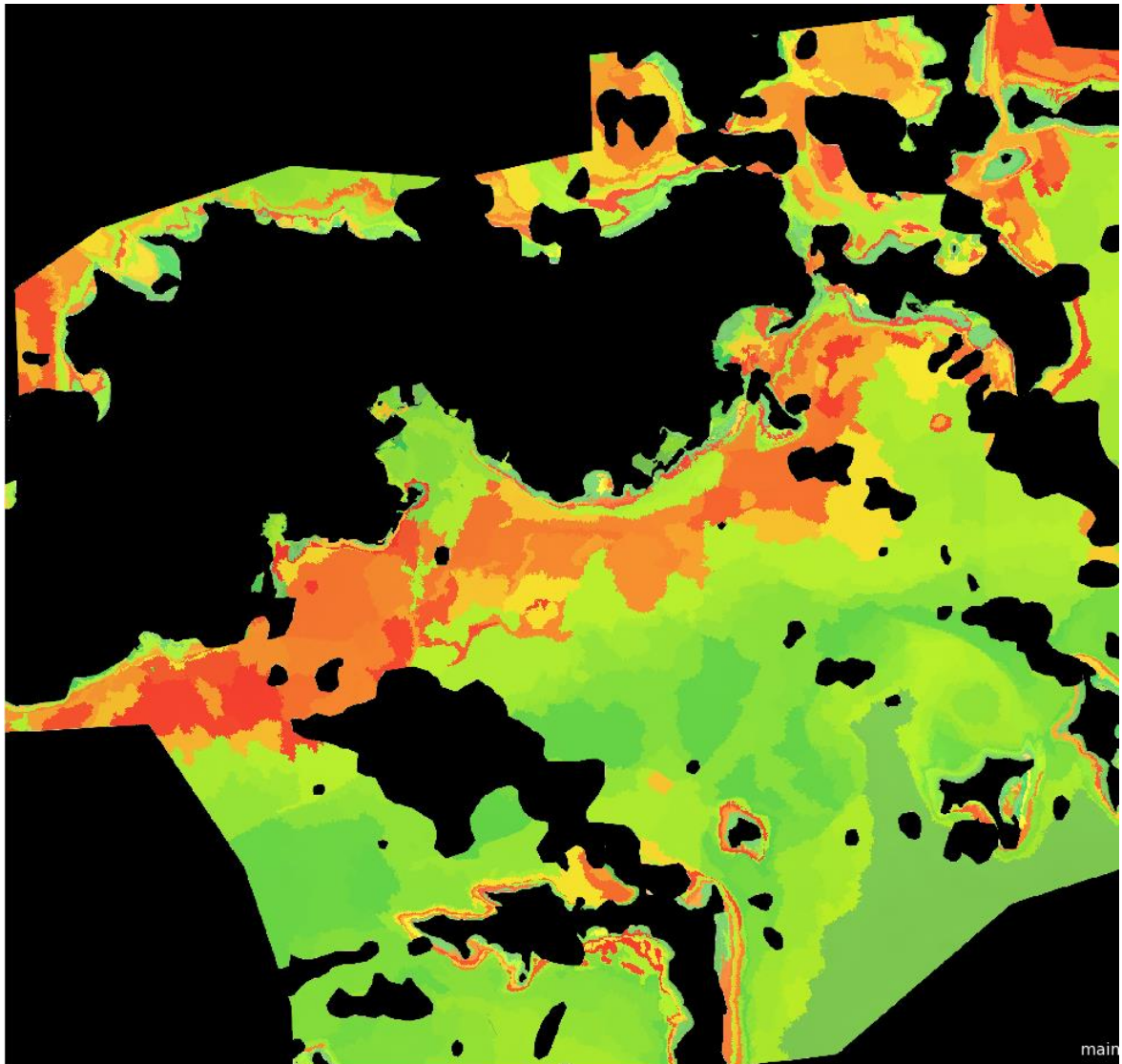


Figure C:2: Post-Irma habitat classification stability for reference image P001.